Gastroenterology 2023;164:72–88

Molecular Markers of Response to Anti-PD1 Therapy in Advanced Hepatocellular Carcinoma

Philipp K. Haber,[1,2] Florian Castet,[3] Miguel Torres-Martin,[3] Carmen Andreu-Oller,[1] Marc Puigvehí,[1,4] Maeda Miho,[1] Pompilia Radu,[5] Jean-Francois Dufour,[5,6] Chris Verslype,[7] Carolin Zimpel,[8,9] Jens U. Marquardt,[8,9] Peter R. Galle,[8] Arndt Vogel,[10] Melanie Bathon,[10] Tim Meyer,[11] Ismail Labgaa,[12] Antonia Digklia,[13] Lewis R. Roberts,[14] Mohamed A. Mohamed Ali,[14] Beatriz Mínguez,[15] Davide Citterio,[16] Vincenzo Mazzaferro,[16] Fabian Finkelmeier,[17] Jörg Trojan,[17] Burcin Özdirik,[18] Tobias Müller,[18] Moritz Schmelzle,[2,19] Anthony Bejjani,[20] Max W. Sung,[1] Myron E. Schwartz,[1] Richard S. Finn,[20] Swan Thung,[1] Augusto Villanueva,[1] Daniela Sia,[1] and Josep M. Llovet[1,3,21]

[1]Mount Sinai Liver Cancer Program, Division of Liver Diseases, Tisch Cancer Institute at the Icahn School of Medicine at Mount Sinai, New York, New York; Division of Hematology and Medical Oncology, Icahn School of Medicine at Mount Sinai, New York, New York; Department of Surgery, Recanti/Miller Transplant Institute at the Icahn School of Medicine at Mount Sinai, New York, New York; Department of Pathology, Molecular and Cell-Based Medicine, Icahn School of Medicine at Mount Sinai, New York, New York; [2]Department of Surgery, Campus Charité Mitte and Campus Virchow Klinikum, Charité-Universitätsmedizin Berlin, corporate member of Freie Universität Berlin, Humboldt-Universität zu Berlin, and Berlin Institute of Health, Berlin, Germany; [3]Translational Research in Hepatic Oncology, Liver Unit, IDIBAPS, Hospital Clinic, University of Barcelona, Catalonia, Spain; [4]Hepatology Section, Gastroenterology Department, Parc de Salut Mar, IMIM (Hospital del Mar Medical Research Institute), Universitat Autònoma de Barcelona, Barcelona, Spain; [5]University Clinic for Visceral Surgery and Medicine, University of Bern, Inselspital, Bern, Switzerland; [6]Hepatology, Department of Clinical Research, University of Bern, Bern, Switzerland; [7]Department of Gastroenterology and Hepatology, KU Leuven, Leuven, Belgium; [8]Department of Medicine I, University Medical Center of the Johannes-Gutenberg University, Mainz, Germany; [9]Department of Medicine I, University of Lübeck, UKSH – Campus Lübeck, Lübeck, Germany; [10]Department of Gastroenterology, Hepatology and Endocrinology, Hannover Medical School, Hannover, Germany; [11]Department of Oncology, University College London Cancer Institute, London, United Kingdom; [12]Department of Visceral Surgery, Lausanne University Hospital and University of Lausanne, Lausanne, Switzerland; [13]Department of Oncology, Lausanne University Hospital and University of Lausanne, Lausanne, Switzerland; [14]Division of Gastroenterology and Hepatology, Mayo Clinic College of Medicine and Science, Rochester, Minnesota; [15]Liver Unit, Hospital Universitari Vall d'Hebron, Vall d'Hebron Barcelona Hospital Campus, Barcelona, Spain; Liver Diseases Research Group, Vall d'Hebron Institute of Research (VHIR), Vall d'Hebron Barcelona Hospital Campus, Barcelona, Spain; CIBERehd, Universitat Autònoma de Barcelona, Barcelona, Spain; [16]Gastrointestinal Surgery and Liver Transplantation Unit, National Cancer Institute, Department of Oncology, University of Milan, Milan, Italy; [17]Department of Gastroenterology, University Liver and Cancer Centre, Frankfurt, Germany; [18]Department of Hepatology and Gastroenterology, Campus Virchow Klinikum and Campus Charité Mitte, Charité University Medicine Berlin, Berlin, Germany; [19]Department of General, Visceral and Transplant Surgery, Hannover Medical School, Hannover, Germany; [20]Division of Hematology/Oncology, Geffen School of Medicine at UCLA, Los Angeles, California; and [21]Institució Catalana de Recerca i Estudis Avançats, Barcelona, Catalonia, Spain

See editorial on page 15.

BACKGROUND & AIMS: Single-agent anti-PD1 checkpoint inhibitors convey outstanding clinical benefits in a small fraction (~20%) of patients with advanced hepatocellular carcinoma (aHCC) but the molecular mechanisms determining response are unknown. To fill this gap, we herein analyze the molecular and immune traits of aHCC in patients treated with anti-PD1. **METHODS:** Overall, 111 tumor samples from patients with aHCC were obtained from 13 centers before systemic therapies. We performed molecular analysis and immune deconvolution using whole-genome expression data (n = 83), mutational analysis (n = 72), and histologic evaluation with an endpoint of objective response. **RESULTS:** Among 83 patients with transcriptomic data, 28 were treated in frontline, whereas 55 patients were treated after tyrosine kinase inhibitors (TKI) either in second or third line. Responders treated in frontline showed upregulated interferon-γ signaling and major histocompatibility complex II–related antigen presentation. We generated an 11-gene signature *(IFNAP)*, capturing these molecular features, which predicts response and survival in patients treated with anti-PD1 in frontline. The signature was validated in a separate cohort of aHCC and >240 patients with other solid cancer types where it also predicted response and survival. Of note, the same signature was unable to predict response in archival tissue of patients treated with frontline TKIs, highlighting the need for fresh biopsies before immunotherapy. **CONCLUSION:** Interferon signaling and major histocompatibility complex–related genes are key molecular features of HCCs responding to anti-PD1. A novel 11-gene signature predicts response in frontline aHCC, but not in patients pretreated with TKIs. These results must be confirmed in prospective studies and highlights the need for biopsies before immunotherapy to identify biomarkers of response.

Keywords: Hepatocellular Carcinoma; Biomarkers; Predictors of Response; Immunotherapy.

Hepatocellular carcinoma (HCC) is a leading cause of cancer-related mortality globally and incidence rates are on the rise.[1] At advanced stages, where only systemic therapies are effective, outcomes remain dismal. Until recently, the treatment landscape of HCC was dominated by tyrosine kinase inhibitors (TKIs), such as sorafenib[2] and lenvatinib[3] that have been able to convey an improvement in survival for most of the population.

The use of immune checkpoint inhibitors (ICIs) has revolutionized clinical care across cancer types. In HCC, the combination of the anti-PD-L1 agent atezolizumab and the monoclonal antibody bevacizumab (anti–vascular endothelial growth factor) has elicited an outstanding median overall survival (mOS) of 19.2[4] months in patients with advanced HCC (aHCC) (IMbrave150 trial) and is now considered standard of care in frontline.[1,5] Furthermore, new ICI-based combinations are expected to reshape the treatment scenario, such as the combination of durvalumab-tremelimumab,[6] which increases overall survival (OS) relative to sorafenib and cabozantinib-atezolizumab, which increases progression-free survival (PFS).[7] These and other combinations currently under investigation are aimed at enhancing the size of the patient subset that derives a benefit from ICI treatment. In this setting, ICIs are commonly regarded as the driving force in improving outcomes, whereas drugs like bevacizumab are thought to expand the immune-sensitive population.[8] Indeed, immunotherapy as standalone treatment is able to convey meaningful benefits in patients with aHCC: early efficacy results from anti-PD1 inhibitors nivolumab[9] and pembrolizumab[10] demonstrated objective response rates (ORR) between 15% and 20%. These responses lasted beyond 16 months[9] and are expected to elicit a mOS >26 months, thereby outperforming the new standard of care. However, the comparatively small size of this subset failed to drive a significant advantage for the entire population, leading to the failure of phase III trials both in the frontline[11] (vs sorafenib) and second line[12] settings (vs placebo), encouraging the utilization of combination treatments. The molecular mechanisms that determine response to anti-PD1 in HCC remain elusive. Thus, the development of predictive biomarkers of response to ICI has the potential to address several unmet clinical needs: (1) to enhance survival in patients likely to respond to therapy, (2) to reduce the risk of treatment-related adverse effects conveyed through combination drugs like bevacizumab, and (3) maximize efficacious application and thereby cost-effectiveness of different treatments.

To address these needs, we established an international consortium of referral centers to identify biomarkers of response in patients treated with anti-PD1. We analyzed tissue samples from patients subsequently undergoing anti-PD1 treatment for advanced HCC at the histologic, mutational, and gene expression levels. Patients responding to anti-PD1 in frontline showed higher baseline levels of intratumoral inflammatory signaling. We generated a gene expression signature capable of capturing responders and validated it in an independent cohort of patients with aHCC and 4 publicly available datasets of solid cancer types comprising >240 patients. Interestingly, the same signature failed to predict response in patients who were pretreated with TKIs, suggesting that archival tissue may not be appropriate to predict response to immunotherapy in patients previously treated with TKIs, as these drugs may modulate response patterns to second line anti-PD1 therapy. Overall, these findings provide a comprehensive picture of the molecular landscape of patients with aHCC responding to anti-PD1 and define a novel tool for patient selection in future clinical trials.

WHAT YOU NEED TO KNOW

BACKGROUND AND CONTEXT

Only 15% to 20% of patients with advanced hepatocellular carcinoma treated with anti-PD1 exhibit a strong benefit, but an understanding of the molecular underpinnings that would enable precision oncology is still amiss.

NEW FINDINGS

We developed a tissue-based genomic tool to predict response in patients treated with anti-PD1 in frontline. Treatment with tyrosine kinase inhibitors between tissue acquisition and anti-PD1 compromises the predictive ability of this marker.

LIMITATIONS

Due to the absence of serial biopsies, an understanding of how tyrosine kinase inhibitors reshape the tumoral microenvironment to mitigate applicability of biomarkers in patients receiving anti-PD1 in second/third line remains unclear.

IMPACT

We provide a comprehensive molecular characterization of responders to anti-PD1. Discrepancies between patients treated in frontline and in second/third line highlight the need for fresh biopsies directly before anti-PD1.

Materials and Methods

Study Population and Endpoints

Under the umbrella of an international consortium comprising 13 centers in the United States and Europe

Abbreviations used in this paper: **aHCC, advanced hepatocellular carcinoma; HCC, hepatocellular carcinoma; ICI, Immune checkpoint inhibitors; IFNγ, interferon gamma; IFNAP, interferon and antigen-presentation; MHC, major histocompatibility complex; mOS, median overall survival; mRECIST, modified response evaluation criteria in solid tumors; NR, nonresponse; OR, objective response; ORR, objective response rates; OS, overall survival; PD, progressive disease; PFS, progression-free survival; SD, stable disease; TKI, tyrosine kinase inhibitors; Tregs, regulatory T cells.**

Most current article

0016-5085/$36.00
https://doi.org/10.1053/j.gastro.2022.09.005

(Supplementary Table 1), we retrospectively collected samples from 111 patients for this study. Eligible patients were ≥18 years with pathologically confirmed HCC at advanced stage (Barcelona Clinic Liver Cancer stage C) or intermediate stage (stage B) after confirmed progression to locoregional therapies and not amenable to a curative treatment approach. Response assessment was performed at least 2 months after the initiation of anti-PD1 treatment via modified response evaluation criteria in solid tumors (mRECIST[13]) and at least 1 untreated lesion was required for inclusion. Patients had compensated liver function and Eastern Cooperative Oncology Group performance score of 0 to 2, as well as otherwise adequate organ and bone marrow function (white blood cell counts ≥2000/μL, platelets ≥50 × 10^3/μL). All patients had archived tissue available obtained from the resection specimen or at the time of biopsy before systemic therapies and underwent anti-PD1 monotherapy. Patients who had been previously treated with an agent targeting T-cell costimulation or checkpoint pathways (including PD-1/PD-L1) were excluded, as were those receiving anti-PD1 or any other treatment neoadjuvantly before resection or in combination with other systemic or percutaneous treatments. Further exclusion criteria were as follows: history of other malignancies, other diseases expected to severely limit life expectancy, brain metastases, history of hepatic encephalopathy, or clinically significant ascites that required paracentesis. Patients with fibrolamellar HCC, sarcomatoid HCC, or mixed cholangiocarcinoma-HCC were excluded. The present study was conducted in accordance with the Helsinki Declaration and local laws. The institutional review board at each contributing center approved the study protocol. All patients alive at the time of study initiation provided written informed consent enabling use of their archived tissues. Consent for already deceased patients was waived by the local institutional review boards.

Given that different systemic treatments may alter the tumoral microenvironment to the point that it may affect the efficacy of subsequent therapies,[14] we stratified patients according to the treatment line in which they received anti-PD1 (Supplementary Table 2).

The primary endpoint applied for the analysis was best objective response (OR), which was assessed in individual centers using mRECIST criteria defining complete response, partial response, stable disease (SD), and progressive disease (PD).[13] Response was generally assessed 2 to 3 months after therapy start and every 3 months thereafter via either computed tomography scan or magnetic resonance imaging. The secondary endpoints were OS and PFS.

Immunohistochemistry, Transcriptome Analysis, CTNNB1 Analysis, and Molecular Data Availability

See the online Supplementary Materials and Methods.

Statistical Analysis

Analyses were performed using the R statistical package and SPSS 24.0 (SPPS Inc., Chicago, IL). Correlations between clinicopathological data and molecular features were performed in case of categorical data with the χ^2 test, whereas continuous data with nonparametric distribution was assessed by the Wilcoxon rank-sum test. Continuous variables with Gaussian distribution were compared with analysis of variance. Survival analysis was performed with Kaplan-Meier estimates and log-rank test with respect to both OS and PFS as well as a Cox regression model. Biomarkers were considered predictive of response or primary resistance to anti-PD1 therapy when 2-sided $P < .05$.

Results

Baseline Characteristics and Clinical Courses

Among the 111 HCC samples collected for the study, 83 cases had enough tissue available for molecular analysis, met all inclusion criteria, and were thus included in the transcriptomic analysis (Figure 1*A*). The time difference between acquisition of the biological sample and initiation of systemic therapies is depicted in Supplementary Figure 1. Recruited patients were treated with nivolumab (n = 67; 80.7%), pembrolizumab (n = 14; 16.9%), or tislelizumab (n = 2; 2.4%) in either frontline (n = 28) or second (n = 41) or third line (n = 14) (Figure 1*B*). All patient demographics and disease characteristics were well balanced between response types (Table 1). Among the 83 patients, 25 exhibited OR (ORR: 30.1%, 3 complete response, 22 partial response), whereas 21 cases (25.3%) had SD and 37 cases (44.6%) PD as best response. Median time to response was 3.0 months (range 1.7–12.8 months) and responses were very durable with 67% lasting 18 months or longer. Median duration of treatment was 4.9 months, and patients displaying OR had a significantly longer time on therapy than nonresponders (18.2 vs 3.3 months, $P < .001$). In terms of outcome, median follow-up was 12.5 months. Responders did not reach mOS during follow-up, whereas mOS was 19.5 months and 12.5 months for patients achieving SD and PD, respectively ($P < .001$, Figure 1*C*). Likewise, responders had significantly longer PFS compared with patients with either SD or PD (median PFS [mPFS]: 28.8 vs 6.2 vs 2.5 months, $P < .0001$) (Figure 1*D*).

Of the 28 patients in the frontline cohort, 12 exhibited OR (ORR: 42.9%). These patients had, expectedly, a significantly better outcome than nonresponders both in terms of OS and PFS ($P < .005$ and $P < .001$, respectively, Figure 2*A* and *B*). A detailed description of patients treated with anti-PD1 in first line is provided in Supplementary Table 3.

Molecular Features of Patients With HCC Responding to Anti-PD1 in Front Line

Overall, differential expression analysis identified 427 genes significantly upregulated in responders ($P < .01$, Supplementary Table 4), with 140 exhibiting a fold change >1.5. Among these, several genes involved in interferon-γ (IFNγ) signaling (*STAT1, STAT2, IRF1*, $P < .0005$, $P < .05$, $P < .05$, respectively, Figure 2*C*) and antigen presentation were significantly upregulated in responding patients. This was particularly evident for major histocompatibility complex (MHC) class II peptides (*HLA-DRA, HLA-DQA1, HLA-DMA*, $P < .01$, $P < .005$, $P < .05$, Figure 2*C* and *D*). Metagenes capturing activation of IFN- and T-cell receptor signaling as well as antigen processing and presentation

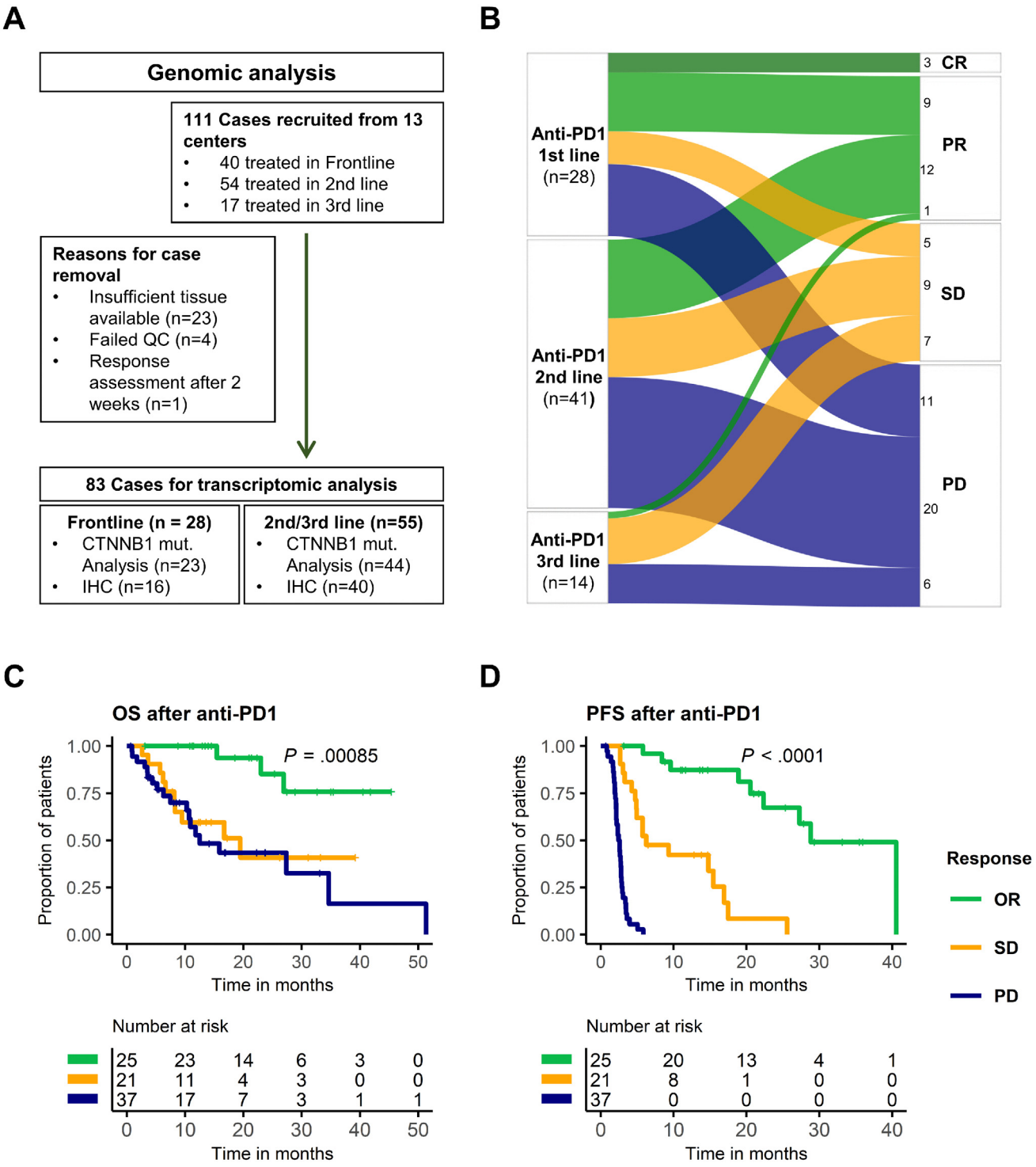

Figure 1. Cohort overview and outcomes. (*A*) Study flowchart: Of the 111 samples collected for this study, 83 cases, treated with anti-PD1 in either frontline or after exposure to TKIs, were eventually included in the transcriptomic analysis. (*B*) Alluvial plot showing response patterns based on treatment line. The numbers in the boxes represent the number of patients with that specific response (*C, D*) Kaplan-Meier (KM) estimates of all patients included in the transcriptomic analysis are shown for OS (*C*) and PFS (*D*) based on whether patients exhibited OR, SD, or PD. *P* values in KM curves represent log-rank tests.

were, likewise, enriched among responders (false discovery rate <0.001). The same patients showed a significant upregulation in the expression of key cytokines involved in chemotaxis (*CXCL9*, *IL18*, $P < .005$ and $P < .001$, respectively). Gene Ontology Enrichment Analysis of the top 140 differentially expressed genes confirmed IFNγ signaling, MHC-II assembly and MHC-II–dependent antigen presentation as the most overexpressed pathways among responders (Figure 2*E*, Supplementary Figure 2*A*). Gene set enrichment analysis using the Hallmark gene sets confirmed enhanced

Table 1. Baseline Characteristics of the Study Population Stratified According to Response Status

Characteristics	All (n = 83)	OR (n = 25)	SD (n = 21)	PD (n = 37)	*P*
Median age, *y* (range)	66 (22–86)	65 (29–86)	63 (22–79)	66 (28–83)	.79
Gender, male, n (%)	65 (77.1)	21 (84.0)	17 (81.0)	26 (70.3)	.4
Etiology, n (%)					
HBV	16 (19.3)	8 (32.0)	3 (14.3)	5 (13.5)	.16
HCV	24 (28.9)	6 (24.0)	7 (33.3)	11 (29.7)	.78
NASH	13 (15.7)	5 (20.0)	4 (19.0)	4 (10.8)	.79
Other Uninfected	31 (37.3)	7 (28.0)	7 (33.3)	17 (45.9)	.323
Child Pugh Score, n (%)[a]					.45
A	72 (88.9)	20 (83.3)	20 (95.2)	32 (88.9)	
B	9 (11.1)	4 (16.7)	1 (4.8)	4 (11.1)	
Fibrosis F3/F4[b]	25 (48.1)	10 (55.6)	7 (50.0)	8 (40.0)	.62
Platelets <100,000/mm^3 (%)[c]	17 (21.3)	4 (16.7)	6 (28.6)	7 (20.0)	.61
BCLC stage, n (%)					.35
Intermediate (B)	17 (20.5)	3 (12.0)	4 (19.0)	10 (27.0)	
Advanced (C)	66 (79.5)	22 (88.0)	17 (81.0)	28 (73.0)	
Macrovascular invasion, n (%)[d]	23 (28.0)	10 (40.0)	6 (28.6)	7 (19.4)	.21
Extrahepatic disease, n (%)	53 (63.9)	17 (68.0)	14 (66.7)	22 (59.5)	.75
Sample origin, n (%)					.12
Primary tumor	73 (88.0)	22 (88.0)	16 (76.2)	35 (94.6)	
Metastasis	10 (12.0)	3 (12.0)	5 (23.8)	2 (5.4)	
Specimen type, n (%)					.61
Resection	49 (59.0)	14 (56.0)	11 (52.4)	24 (64.9)	
Biopsy	34 (41.0)	11 (44.0)	10 (47.6)	13 (35.1)	
AFP (ng/mL) >200, n (%)[d]	30 (36.6)	7 (28.0)	10 (47.6)	13 (36.1)	.39
Anti-PD1 drug, n (%)					.67
Nivolumab	67 (80.7)	19 (76.0)	16 (76.2)	32 (86.5)	
Pembrolizumab	14 (16.9)	5 (20.0)	4 (19.0)	5 (13.5)	
Tislelizumab	2 (2.4)	1 (4.0)	1 (4.8)	0 (0)	
Median time on therapy in month (range)	4.9 (0.47–45.4)	18.2 (3.1–45.4)	4.9 (0.5–25.7)	2.3 (0.47–33.6)	<.001
Events					
Deceased	32 (38.6)	3 (12.0)	10 (47.6)	19 (51.4)	<.01
Progression	58 (69.9)	8 (32.0)	14 (66.7)	37 (100)	<.001
Median time to response in months (range)[e]		3 (1.7–12.8)			

AFP, alpha fetoprotein; BCLC, Barcelona Clinic Liver Cancer; HBV, hepatitis B virus; HCV, hepatitis C virus; NASH, nonalcoholic steatohepatitis.
[a]Data missing from 2 cases.
[b]Data missing from 31 cases.
[c]Data missing from 3 cases.
[d]Data missing from 1 case.
[e]Data missing from 7 cases.

IFN-signaling in responders (false discovery rate <0.001, Supplementary Table 5, Supplementary Figure 2*B*). Comparison between patients exhibiting disease control (disease control rate = OR + SD) and those with PD revealed a significant enrichment in *CD274* (PD-L1) expression in disease control rate patients, although no difference was observed in PD-L1 staining by immunohistochemistry, a discrepancy previously characterized.[15] Likewise, gene expression of *PDCD1LG2* (PD-L2), the alternative ligand to PD-1, was significantly higher in responders ($P < .01$), whereas expression of its common receptor *PDCD1* (PD1) was markedly increased among patients with PD ($P < .05$) (Figure 2*C*).

We next sought to correlate clinical response to anti-PD1 therapy with previously established molecular classes of HCC (Figure 3*A*), including the recently characterized HCC *Inflamed class*,[16] which further refines our previously published *Immune class* of HCC.[17] The inflamed class entails 3 subtypes, named *Active, Exhausted,* and *Immune-like* that all share a microenvironment with increased IFN-signaling.

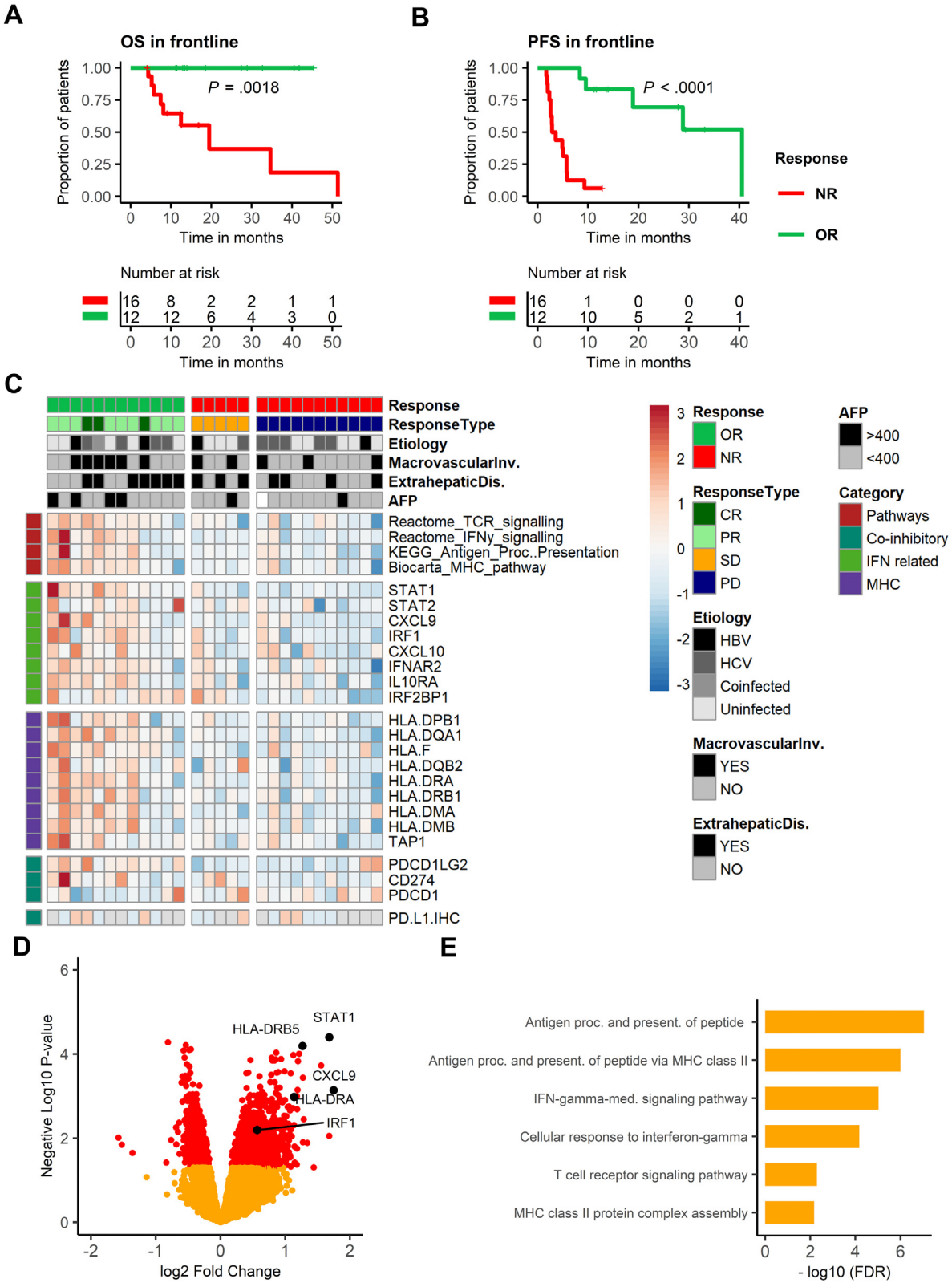

Figure 2. Upregulation of inflammation and antigen-presentation associated genes in responders. (*A, B*) Kaplan-Meier (KM) estimates for OS (*A*) and PFS for all 28 patients treated with anti-PD1 in frontline based on whether patients exhibited OR or NR. (*C*) Heatmap of gene expression analysis based on observed response types. Each signature or individual gene is significantly upregulated in one response subgroup relative to the others, whereas no differences were observed regarding PD-L1 by immunohistochemistry. (*D*) Volcano plot showing differentially expressed genes in responders compared with nonresponders. Genes differentially expressed at $P < .05$ are depicted in red, all others in orange. (*E*) Gene Ontology gene set enrichment analysis of differentially expressed genes using the *biological processes* classification. *P* values in KM curves represent log-rank tests.

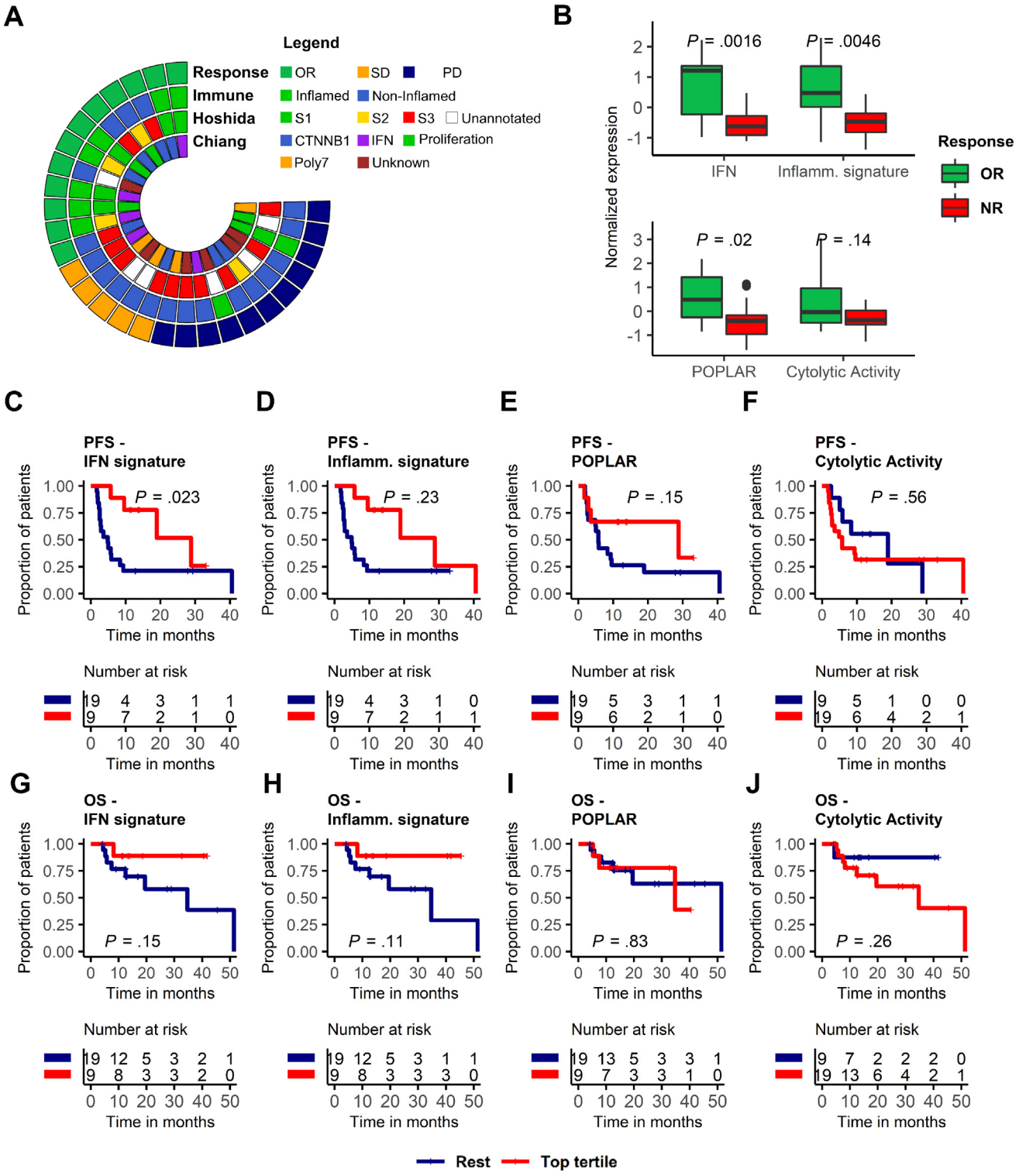

Figure 3. Association of previously reported gene signatures and HCC molecular classes with response and resistance to anti-PD1. (*A*) Circular classification plot integrating response types with molecular classes of HCC. Each sector represents 1 patient. Significant enrichment of the *S1/2* classes and the *Inflamed HCC* subgroup is observed in responders. (*B*) Boxplot comparison for the expression of previously reported gene signatures based on observed response. (*C–J*) Kaplan-Meier (KM) estimates for PFS (*C–F*) and OS (*G–J*) based on expression of previously reported signatures. *P* values in boxplot comparison represent Mann-Whitney test, and those in the KM curves represent log-rank tests.

Interestingly, patients belonging to the HCC *Inflamed class* showed a higher rate of OR compared with the other classes *Intermediate* and *Excluded* (7 of 9 vs 5 of 19, $P = .01$), whereas differences in PFS showed a nonsignificant trend ($P = .068$, Supplementary Figure 2*C*). Patients with an aggressive and proliferative HCC phenotype (classes *S1* and *S2)* had markedly longer PFS when treated with anti-PD1 compared with the rest ($P = .017$, Supplementary Figure 2*D*). Next, we evaluated previously reported signatures and biomarkers of response to anti-PD1 therapy in our dataset (Supplementary Table 6). Interestingly, we observed that several signatures, such as the *IFN signature,*[18] *POPLAR,*[19] and the *Inflammatory signature,*[20] were significantly enriched in HCC responding patients ($P < .01$, $P < .01$, $P < .05$, respectively, Figure 3*B*). In terms of outcome, both *IFN-* and the *Inflammatory signature* were associated with longer PFS ($P = .023$ for both, Figure 3*C* and *D*), whereas no differences were observed for *POPLAR* or the *cytolytic activity* signature (Figure 3*E* and *F*). However, none of the signatures was able to predict significantly longer OS (Figure 3*G–J*). A summary of the performance of these signatures is provided in Supplementary Table 7. When considering histologic markers, such as the richness of the immune infiltrate, Tertiary lymphoid structures signature,[21] and PD-L1 expression, as well as tumor mutational burden inferred through a gene signature,[22] no positive correlation with response to ICIs was observed (Supplementary Figure 3*A* and *C*).

A Novel 11-Genes Signature Accurately Predicts Response to Anti-PD1

Given the paucity of studies identifying candidate biomarkers for anti-PD1 in HCC and that none of the previously reported signatures was able to predict both PFS and OS, we then developed a gene expression signature capable of discriminating responding from nonresponding patients (see Supplementary Methods). The resulting 11-gene set, hereafter named *IFNAP signature* (interferon and antigen presentation, Supplementary Table 8), comprises genes involved in IFN-γ signaling (*STAT1, GBP1*), antigen presentation (*B2M, HLA-DRB5, HLA-DRA*), and chemotaxis (*CXCL9*, Figure 4*A*). Most of these genes were not shared with other published immune response signatures (Supplementary Figure 4*B*), underscoring the unique composition of IFNAP. The IFN signature and IFNAP shared 3 individual genes, all of which were predictive of OR and PFS. Likewise, the non-overlapping genes in IFNAP were linked with OR and PFS, whereas the remaining genes in the IFN signature were not (Supplementary Figure 5*A–C*). Patients with high expression of IFNAP (n = 9, defined as those within the upper tertile, see Supplementary Methods) had superior outcomes both with regard to PFS ($P = .035$) and OS ($P = .039$, Figure 4*B* and *C*). Receiver operating characteristic analysis indeed revealed IFNAP as the most efficient geneset at discriminating responding from nonresponding patients with an area under the curve of 0.87 (Figure 4*D*).

We next sought to investigate the robustness of the IFNAP signature by testing its stability across different regions within a given tumor to investigate whether intratumoral heterogeneity, which may cause differences in regional adaptive immune responses, may compromise the reproducibility of signature expression. For this purpose, we re-analyzed a cohort published by our group including 30 HCC samples from 15 patients with tumors >4 cm,[23] and we found expression between 2 distinct regions of the same tumor to be very stable and 90% of cases had the same expression category (low/high) in both samples. Indeed, correlation of IFNAP between 2 regions of a given tumor was significant (R = 0.77, $P < .001$, Supplementary Figure 4*C*).

We tested IFNAP in 4 independent datasets (see Supplementary Methods) comprising 240 patients with non–small-cell lung cancer,[24,25] head and neck squamous cell carcinoma,[24] or melanoma[24,26,27] treated with anti-PD1/anti-PD-L1. In the first dataset,[24] patients with OR had significantly more often high IFNAP expression, which was, moreover, associated with longer mPFS (55% vs 24.4%, $P = .017$, and 6.9 vs 2.8 months, $P = .039$, respectively, Figure 4*E–H*). Likewise, in the second dataset,[25] high IFNAP expression was associated with response and longer mPFS (75% vs 15.8%, $P = .006$ and 8.6 vs 1.2 months, $P = .006$, respectively, Figure 4*G* and *H*). In the third dataset,[27] OR was again associated with high IFNAP expression (42.5% vs 27.4%, $P = .043$, Supplementary Figure 6*A*), which in turn predicted longer mPFS and mOS (13.3 vs 3.2 months, $P = .011$ and nonresponse (NR) vs 19.7 months, $P = .033$, respectively, Supplementary Figure 6*B* and *C*). Finally, IFNAP also predicted higher response (46.7% vs 15.6%, $P = .039$, Supplementary Figure 6*M*) in the fourth dataset.[26] Of note, none of the previously published signatures consistently predicted response or PFS in any of the datasets (Supplementary Figure 6*D–L* and *N–P* and Supplementary Figure 7*A–F* and *I–L*), with the exception of the *IFN signature* in the Jung et al[25] dataset (Supplementary Figure 7*G* and *H*). In summary, the IFNAP signature was able to capture responders to anti-PD1 pretreatment across cancer types and was associated with longer PFS and OS, whereas none of the previously published signatures was capable of consistently eliciting the same significant differences. This is of note, as several of these signatures were designed in tumors that are investigated in the validation datasets.[18,19] In these, patients were treated with anti-PD1 both in frontline as well as in second line. However, unlike in our cohort, none of the patients underwent TKI treatment before immunotherapy and most tissue samples were obtained directly before the initiation of anti-PD1 therapy.

Finally, we tested the ability of IFNAP to predict response and longer survival in a dataset of patients treated with either single-agent ICI (n = 13, nivolumab) or combination treatment (nivolumab/ipilimumab or spartalizumab/sabatolimab, n = 11).[28] High expression of IFNAP assessed by nanostring was associated with significantly longer OS and a trend toward higher OR (Supplementary Figure 8*A* and *B*) to nivolumab but not to combination treatment (Supplementary Figure 8*C* and *D*), suggesting molecularly distinct mechanisms of response for the combination.

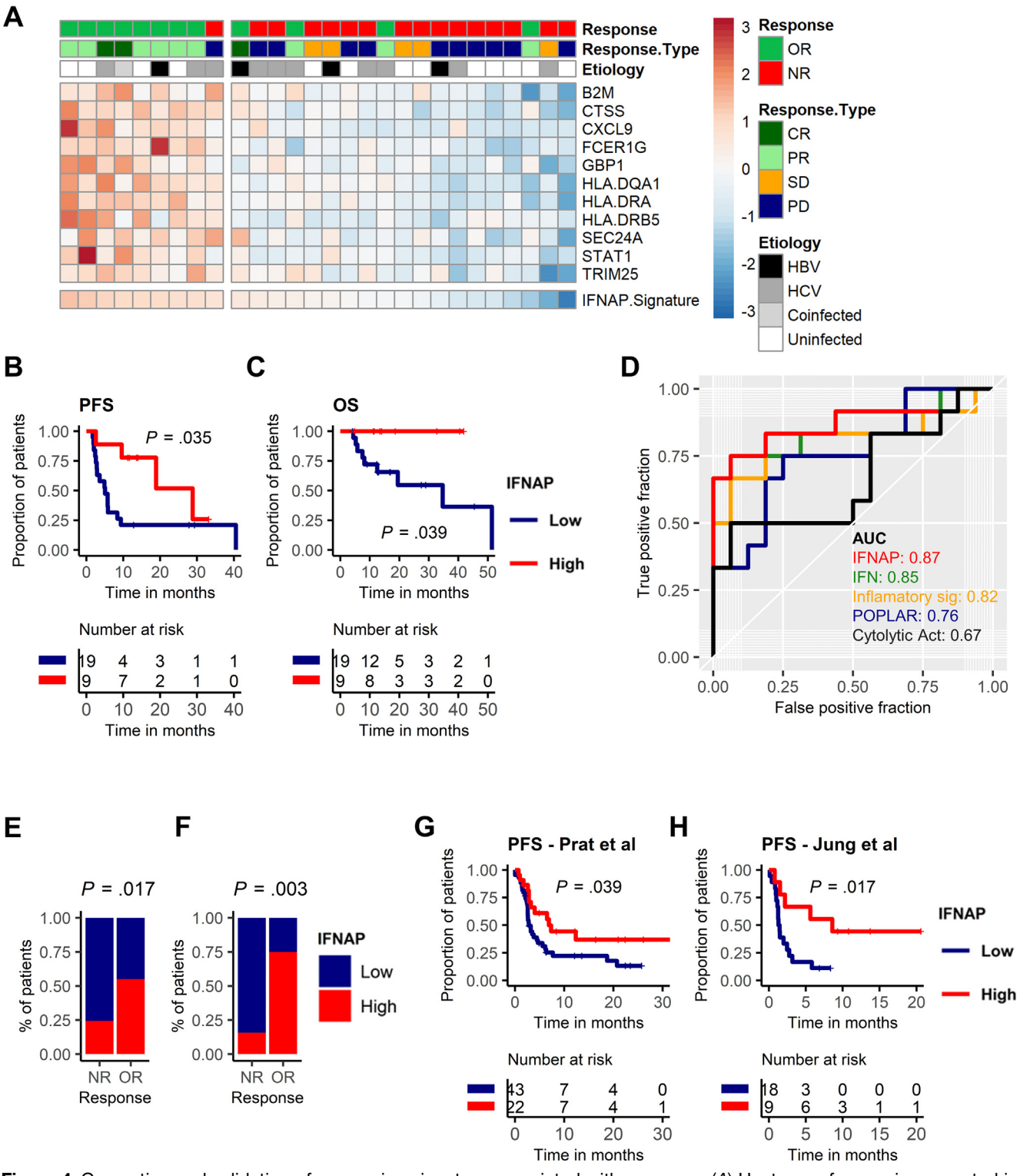

Figure 4. Generation and validation of expression signature associated with response. (*A*) Heatmap of genes incorporated in the IFNAP signature. (*B, C*) Kaplan-Meier (KM) estimates for PFS (*B*) and OS (*C*) are shown based on expression of IFNAP. (*D*) Receiver operating characteristic (ROC) curve is shown for IFNAP and previously characterized signatures of response. AUC, area under the curve. (*E, F*) Validation of IFNAP in 2 independent datasets of anti-PD1/anti-PDL1-treated patients with melanoma, non–small-cell lung cancer (NSCLC) and head and neck squamous cell cancer (*E, G*) and NSCLC (*F, H*), respectively. Patients with response showed marked enrichment in IFNAP (*E, F*) which was associated with longer PFS (*G, H*). *P* values for KM analysis derive from log-rank test whereas those in the barplots represent 2-sided χ^2 test.

The IFNAP Gene Signature Captures a Unique Immune Microenvironment

Because the increased expression of IFN- and antigen presentation–related genes is not unequivocally associated with a specific cell type but can be conferred through both tumoral and immune cells, we next characterized the immune infiltration in patients with high IFNAP expression. Strikingly, patients with high and low IFNAP expression were not different in terms of actual immune cell infiltration quantified on hematoxylin-eosin–stained slides (see the Materials and Methods section) both in the intratumoral area and at the invasive margin (Figure 5*A*). We next hypothesized that the microenvironmental composition rather than overall infiltration may drive response to anti-PD1 in HCC. Thus, we performed virtual microdissection using CIBERSORTx[29] and found a significant upregulation of plasma cells, CD4-memory activated T cells and M1 macrophages in patients with high expression of IFNAP (Figure 5*B*, Supplementary Figure 9). Conversely, patients with low IFNAP showed a significant increase in the infiltration of immunosuppressive regulatory T cells (Tregs, $P = .001$). Indeed, expression of IFNAP showed a negative correlation with expression of Tregs and of Forkhead-Box-Protein P3 (*FOXP3*, Figure 5*C*), a transcription factor active in Tregs that has been previously implicated in driving immunosuppression across cancer types and is linked with hyperprogression after anti-PD1.[30] In our dataset, low expression of Tregs or IFNAP, defined by the first tertile, was associated with markedly lower PFS (4.9 vs NR and 3.6 vs 28.8 months, $P = .012$ and $P < .001$, respectively, data not shown). We also considered other features associated with primary resistance to anti-PD1 and found significant negative correlations between IFNAP and *PDCD1* expression (Figure 5*C*). Interestingly, all these markers of immunosuppression were highly correlated with each other and were negatively correlated to all genes of the IFNAP signature (Pearson correlation, Figure 5*D*). Overall, these data indicate that immunosuppressive expression programs predict poor outcome after anti-PD1 therapy. The presence of Tregs in the microenvironment may be one of the key factors eventually driving resistance, whereas the other factors could represent downstream effects of this microenvironmental composition.

CTNNB1 Mutational Status Is Not a Dominant Feature to Predict Resistance to Anti-PD1 Therapy

Mutations in the WNT-CTNNB1 pathway have been implicated in driving resistance in a murine model of HCC.[31] We then investigated whether the presence of *CTNNB1* mutations was able to predict primary resistance to anti-PD1. To this end, we correlated treatment response with tumoral mutational status in 23 cases of frontline-treated patients. We found 4 of 11 responders (36%) and 6 of 12 nonresponders (50%) to have mutations in exon 3 of *CTNNB1*, the dominant hotspot, thereby showing no significant differences in response rates (Figure 5*E*). We considered that patients with *CTNNB1* exhibited less-durable responses than nonmutated patients, but no differences were observed in PFS and OS. Likewise, no difference in PFS and OS was seen among nonresponding patients based on mutational status (Supplementary Figure 10). Next, we compared the gene expression profile of *CTNNB1*-mutated patients who exhibited response (n = 4) with those patients with mutations who did not (n = 6). We observed a trend toward increased inflammatory signaling as captured by the cytolytic activity gene signature[32] in those patients with mutations who responded. Moreover, the same patient subset demonstrated an upregulation in genes associated with an active immune response (*GZMA, CXCL9*; 1-sided $P < .05$).

In summary, *CTNNB1* mutational status did not predict resistance to therapy. A trend toward more inflammatory signaling in responders despite the presence of mutations hints at a more intricate role of *CTNNB1* in this scenario. Although previous studies have shown discrepancies in terms of the role of *CTNNB1* as a driver of immune exclusion,[31,33,34] our findings provide an explanation to reconcile these inconsistencies. Indeed, our data suggest that patients with *CTNNB1*-driven immune exclusion may be prone to resistance. However, in tumors in which this profile is overcome by unknown mechanisms to establish an inflamed microenvironment, the conducive effects of IFN-signaling and the intact antigen-presenting machinery may outweigh the impact of *CTNNB1* mutations.

Prior Treatment With TKIs May Influence Response to Subsequent Anti-PD1 in Second Line

Overall, 55 patients underwent anti-PD1 treatment as second (41 cases) or third line (14 cases) therapy after previous exposure to TKIs (54 sorafenib, 1 lenvatinib, Supplementary Table 9). In all but 2 of these cases, though, histology was obtained before first-line therapy. Overall, the ORR was 23.6%, and as in frontline-treated patients, responders had both markedly longer OS and PFS ($P = .047$ and $P < .0001$, respectively, Figure 6*A* and *B*). In this setting, neither IFNAP (n = 18 patients in second/third line) nor other previously reported signatures were significantly enriched among patients with OR (Figure 6*C*, Supplementary Figure 11*A*, *D*, *G*, and *J*). This translated to clinical outcome, where no differences were observed between patients with high and low expression of these signatures (Supplementary Figure 11*B, C, E, F, H, I, K*, and *L*). Likewise, histologic severity of the immune infiltrate and inferred presence of Tertiary lymphoid structures signature[21] and high tumor mutational burden were not linked to response in patients treated with anti-PD1 in second line either (Supplementary Figure 3*B* and *C*).

We thus considered that TKIs may affect the success of subsequent anti-PD1 therapy in a way that renders some tumors that would be expected to respond to anti-PD1 in frontline no longer responsive after prior TKI therapy. Conversely, a subset of tumors that would be expected to exhibit resistance to anti-PD1 when treated in frontline did respond when pretreated with TKIs. In an exploratory analysis, we investigated factors that may guide whether or not TKI therapy is conducive for subsequent anti-PD1

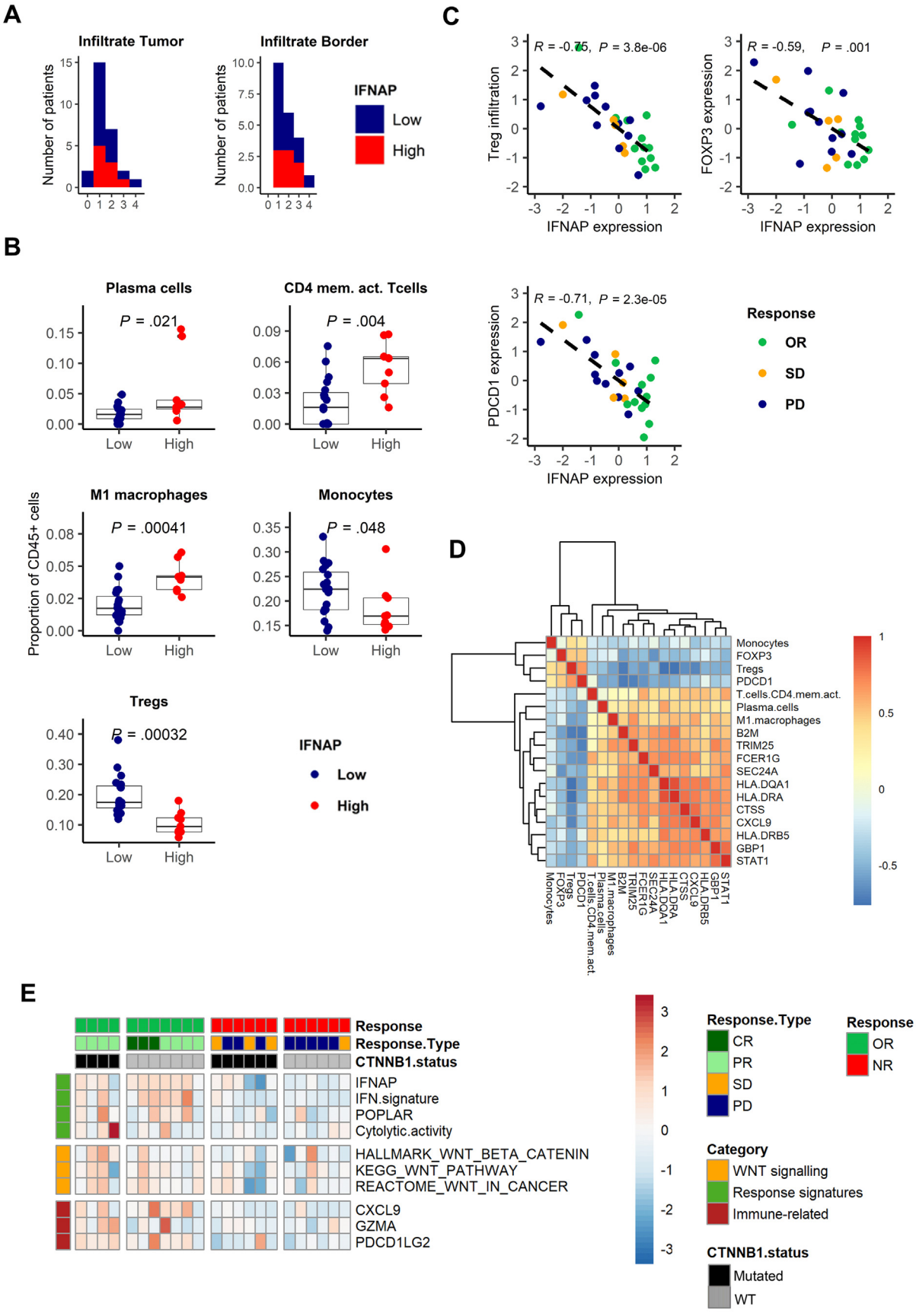
A
Infiltrate Tumor
Infiltrate Border
Number of patients
IFNAP
Low
High
B
Plasma cells
P = .021
CD4 mem. act. Tcells
P = .004
M1 macrophages
P = .00041
Monocytes
P = .048
Tregs
P = .00032
Proportion of CD45+ cells
C
R = -0.75, P = 3.8e-06
Treg infiltration
IFNAP expression
R = -0.59, P = .001
FOXP3 expression
R = -0.71, P = 2.3e-05
PDCD1 expression
Response
OR
SD
PD
D
Monocytes
FOXP3
Tregs
PDCD1
T.cells.CD4.mem.act.
Plasma.cells
M1.macrophages
B2M
TRIM25
FCER1G
SEC24A
HLA.DQA1
HLA.DRA
CTSS
CXCL9
HLA.DRB5
GBP1
STAT1
E
Response
Response.Type
CTNNB1.status
IFNAP
IFN.signature
POPLAR
Cytolytic.activity
HALLMARK_WNT_BETA_CATENIN
KEGG_WNT_PATHWAY
REACTOME_WNT_IN_CANCER
CXCL9
GZMA
PDCD1LG2
Response.Type
CR
PR
SD
PD
Response
OR
NR
Category
WNT signalling
Response signatures
Immune-related
CTNNB1.status
Mutated
WT

treatment. Patients with low inflammatory signaling and resistance to therapy (IFNAP low NR) showed an upregulation in metabolic signaling pathways compared with patients with low inflammatory signaling who did respond (IFNAP low OR, Supplementary Figure 12*B*) and retained the significant enrichment in Tregs infiltration by CIBERSORTx (Supplementary Figure 12*C*). Conversely, patients with low IFNAP expression and response showed a marked increase in CD4 naïve T-cell infiltration. Overall, these data suggested that severe infiltration of regulatory T cells may impede anti-PD1–mediated antitumoral immunity even after TKI therapy, as this feature was maintained both in frontline and second/third line treated patients. Indeed, markedly worse PFS was observed in the top 20% of patients who harbored the highest infiltration in Tregs in both frontline and second/third line (Figure 6*C*–*E*). This same subset of patients presented a significant enrichment in the expression of *SOCS1* and *SOCS3*, key antagonists of JAK/STAT signaling and thus inhibitors of the intracellular IFN-response pathway (Figure 6*C*). In keeping with this, the same subset featured significant downregulation in key genes involved in IFN-signaling and an active antigen-presenting machinery.

In the absence of human datasets featuring serial biopsies to investigate the distinct effect of TKIs on the tumoral microenvironment, we explored a recently published murine model in which HCC-bearing mice were treated with either lenvatinib or placebo (Supplementary Figure 12*D*, see Supplementary Methods). Comparative gene expression analysis of mice treated with lenvatinib for 2 weeks revealed a significant enrichment in inflammatory signaling by TKIs as captured by higher expression of IFNAP and the IFN signatures (Supplementary Figure 12*E*). Cellular subsets, such as CD4 effector memory cells, that we linked to response to anti-PD1, were, likewise, upregulated after lenvatinib treatment. Overall these data suggest that TKIs may modulate response to anti-PD1 by altering microenvironmental signaling.

Overall, our findings suggest that fresh tissue should be obtained directly before the initiation of a given treatment to enable precision oncology, as prior lines of systemic therapy compromise the readout quality of biomarkers. Our data indicate a patient subset, characterized through severe Treg infiltration and overexpression of immune-evasion–related genes that is linked to poor outcomes when treated with anti-PD1 both in frontline as well as in second/third line.

Discussion

The present study represents a comprehensive characterization of the molecular patterns associated with response and resistance in patients with advanced HCC treated with anti-PD1. Herein, we identified IFN-signaling and antigen-presentation–related genes to be associated with OR, whereas presence of Tregs and pathways associated with immunosuppression are linked to resistance. We developed an 11-gene expression signature capable of predicting response to anti-PD1 in HCC and other solid cancer types when treated with anti-PD1 in the frontline setting. When testing the signature in samples from patients pretreated with TKIs, we found that neither our signature nor previously reported inflammatory markers predict outcomes to second or third line anti-PD1 therapy, suggesting that prior lines of therapy may affect the efficacy of subsequent anti-PD1.

In recent years, several predictive biomarkers of response and resistance to systemic therapies have entered the clinical space. Regarding anti-PD1 therapy, the only biomarkers approved by the Food and Drug Administration are high tumor mutational burden and microsatellite-instability across cancer types. The benefit conveyed by these biomarkers is limited in magnitude (<3% of HCCs), underscoring the need for more refined testing. Earlier studies in melanoma and lung cancer have observed an increase in T-cell infiltration in the tumor microenvironment and enrichment of IFNγ-signaling in patients responding to anti-PD1 therapy.[18,19] Although this observation has been consistently confirmed in early on-treatment samples collected 2 to 4 weeks after therapy start,[35] results in samples collected before the initiation of therapy are conflicting.[26]

Among the most relevant findings of our study, we identified a gene expression signature—IFNAP—that predicts response and survival to frontline anti-PD1 in aHCC. Notably, it outperformed previously published signatures of response and was the only one to predict significant increases in ORR, OS, and PFS in our dataset, as well as in an aHCC validation cohort and 4 expression datasets from other solid cancer types across different platforms (Nanostring, microarray, RNA-sequencing). IFNAP identified responders independent of the etiology of the underlying liver disease, in which 4 of 5 responders without viral hepatitis had high expression of the signature. This is particularly relevant in light of a recently published report that draws the efficacy of anti-PD1 therapy in patients with nonalcoholic steatohepatitis into question.[36] The composition of IFNAP reflects key biological pathways involved in T-cell–directed therapies: (1) IFN-signaling and (2) antigen-presentation, which are readouts of nascent cancer cell immunogenicity, that can be leveraged through immunotherapy.[18] IFNAP includes genes such as *B2M*, whose loss of heterozygosity has been implicated as a mechanism of

Figure 5. Characterization of IFNAP and correlates of resistance to anti-PD1. (*A*) Histologic assessment of the immune infiltrate, applying a previously characterized semi-quantitative score,[17] in the intratumoral compartment and at the invasive margin. (*B*) Boxplot representation of virtual microdissection with CIBERSORTx based on IFNAP expression. (*C*) Correlation of IFNAP expression with previously characterized resistance markers. (*D*) Correlation heatmap with unsupervised clustering of factors associated with response and resistance to anti-PD1 therapy. (*E*) Heatmap of patients treated in frontline with anti-PD1 ordered by response and CTNNB1 mutational status. No differences in response rates were observed, whereas a trend toward increased inflammatory signaling in responders with CTNNB1 mutations compared with nonresponders with mutations was noted. *P* values in boxplot comparison represents Mann-Whitney test, and those in the correlation plots represent Pearson tests.

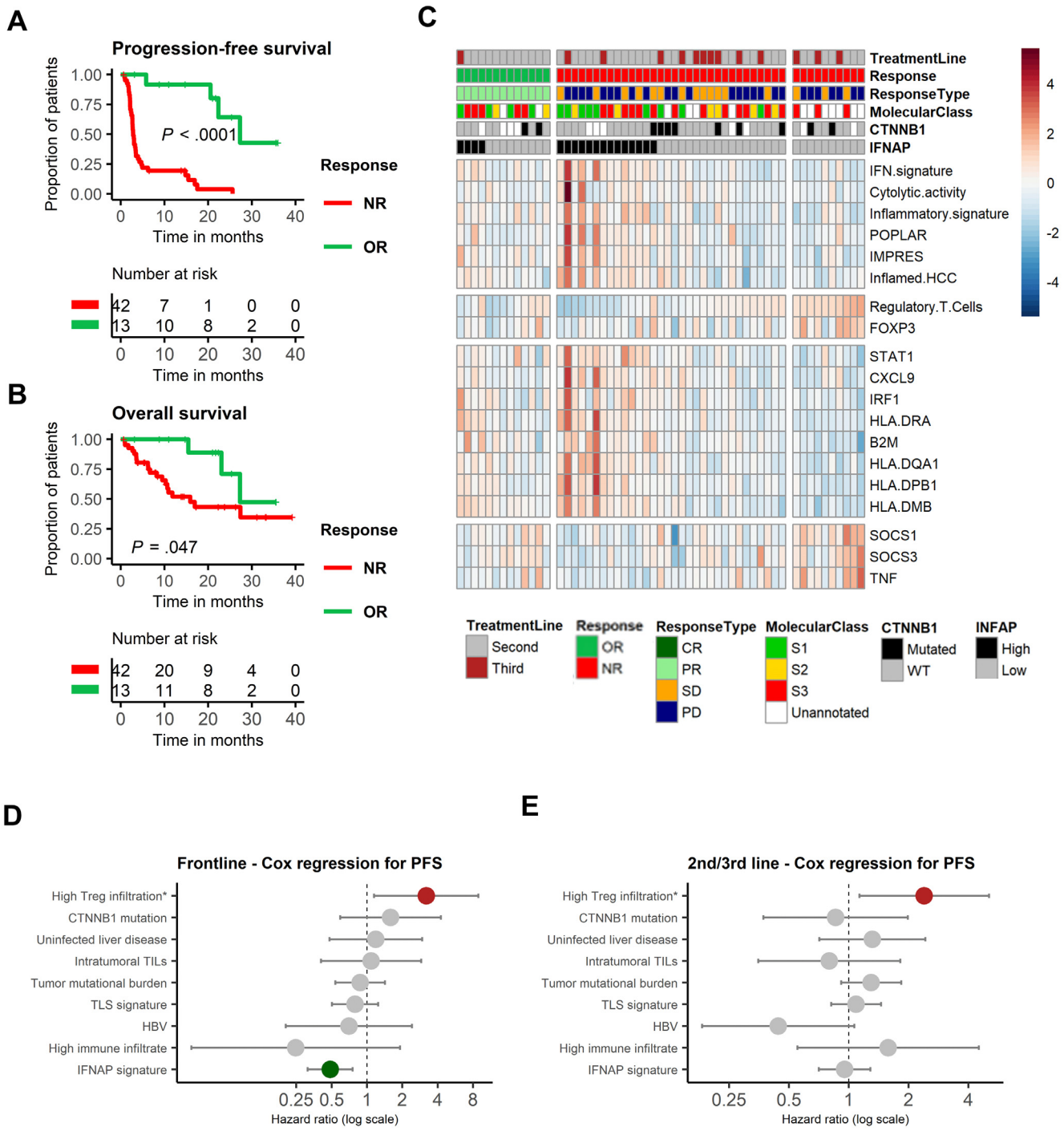

Figure 6. TKI therapy compromises predictive potential of response signatures. (*A, B*) Kaplan-Meier estimates for PFS and OS in patients treated with anti-PD1 in second/third line. (*C*) Heatmap of patients treated with anti-PD1 in second and third line highlights inability of previously characterized markers to capture responders to anti-PD1 after TKI therapy. (*D, E*) Forest plots showing log hazard ratios from a Cox regression model for PFS defines high infiltration of Tregs (Top 20%) as a poor prognostic marker in patients treated with anti-PD1 both in frontline (*D*) and after exposure to TKIs (*E*). *P* values in Kaplan-Meier curves represent a log-rank test.

resistance to anti-PD1,[37] and *CXCL9* as well *HLA-DRA* that have been linked to response in melanoma.[18] In our dataset, analysis of the immune infiltrate suggested that the composition rather than overall infiltrate might drive response to immunotherapy. Specifically, CD4+ naïve T cells were consistently upregulated in patients with high IFNAP expression, whereas Treg infiltration was negatively correlated with IFNAP. The presence of immunosuppressive Tregs and their active transcription factor *FOXP3* may in this regard be an impediment toward initiating antitumoral immunity. A recent biomarker analysis of patients with HCC treated with atezolizumab and bevacizumab in clinical trials

identified that increased IFNγ-signaling, active antigen-presentation, and low Treg/Effector-T-cell ratio were linked to response. In addition, patients with high Treg infiltration experienced a significantly stronger benefit from combination compared with atezolizumab monotherapy, suggesting synchronous application of ICI with anti-angiogenics may help in overcoming severe Treg infiltration as a driver of resistance to ICI monotherapy.[38]

Several investigations in melanoma have shown genetic alterations in the WNT-CTNNB1 pathway to be a tumor-intrinsic driver of immune exclusion and resistance to anti-PD1.[39] In HCC, a preclinical study suggested that *CTNNB1* mutations conveyed defective recruitment of dendritic cells and subsequently impaired cytotoxic T-cell function.[31] These effects were reverted on overexpression of *CCL5*. One cohort study supported this correlation in patients who underwent biopsy before treatment,[33] whereas another did not identify *CTNNB1* mutations in liquid biopsy affecting PFS.[34] Our results point toward the fact that *CTNNB1* mutations alone are not associated with resistance, although the underlying biological mechanisms remain elusive. Those patients with inflammatory signaling counterbalancing *CTNNB1*-related immunosuppression showed a trend to better OR, as opposed to those in whom *CTNNB1* mutations were the dominant molecular feature determining lack of response to anti-PD1. In the former cases, other signaling pathways such as IFN-signaling and an active antigen-presenting machinery may overcome *CTNNB1*-mediated immune exclusion and thus facilitate response.

Finally, the aforementioned differences in expression profiles between responding and nonresponding patients were no longer evident in those patients receiving TKIs between sample acquisition and immunotherapy start. This finding could be because of the longer time elapsed between tissue acquisition and anti-PD1 treatment in the second/third line when compared with the frontline, which may increase the odds of molecular events contributing to immunosuppression, although this is unlikely given the relative stability of driver events during cancer evolution.[40] An alternative hypothesis would be that treatment with TKIs may influence how a patient responds to anti-PD1 therapy in subsequent treatment lines. In the absence of serial biopsies, the molecular mechanisms that guide the impact of TKIs on other treatments remain unknown, and it is unclear as to whether an inflamed microenvironment pre-sorafenib remains inflamed thereafter or if the effect of the TKI may ameliorate inflammatory signaling in these tumors.

Data from the murine model suggest[41,42] that TKIs may overall increase inflammatory signaling within the tumor and induce a shift in the composition of the microenvironment. However, it needs to be acknowledged that these models are not fully reflective of human disease course because the molecular analyses were performed on animals during TKI treatment, whereas humans are generally not exposed to anti-PD1 before resistance to TKIs. As previous studies have shown that although sorafenib-sensitive tumors display an increase in inflammatory signaling and an enhanced antigen-presentation apparatus, resistance in turn is associated with a less-rich T-cell infiltration and less overall inflammatory signaling within the tumor.[42] Likewise, a recent biomarker companion study for a phase I clinical trial aiming at converting locally advanced disease to resectable HCC through neoadjuvant cabozantinib and nivolumab confirmed heterogeneous expression of TKI targets and inflammatory markers based on response status.[43]

Our data imply that responders in different treatment lines are different populations with some overlap. Conversely, we have identified a subset of patients who exhibit resistance to anti-PD1 regardless of whether treatment is administered in frontline or after exposure to TKIs. This subset was characterized through an increase in Treg infiltration and expression of genes that are direct inhibitors of active JAK/STAT signaling. Overall, our data opens up the enticing perspective that more patients with HCC could respond to anti-PD1 therapy through selective pretreatment/or combination with TKIs, although some patients may not be suitable for anti-PD1 in any case. Our data ultimately calls for the need of biopsies before anti-PD1 treatment start to enable biomarker-based precision oncology regardless of treatment line.

Several limitations of this study need to be addressed: first, the distinction between therapy lines diminishes the sample size considerably and limits the power of the study despite recruitment from 13 international referral centers. The observed response rate of 43% in the first-line cohort is certainly above the expected 15% to 20% response rate and is a reflection of the inclusion criteria of a minimal duration of 2 months of treatment to evaluate response. Although this naturally increases the proportion of responders, it also increases the power of our biomarker analysis. In addition, the use of mRECIST response criteria likely contributes a small further increase in the ORR. Second, the lack of serial biopsies between systemic treatments precludes a refined analysis on how precisely TKI therapy alters the microenvironment and affects efficacy of subsequent immunotherapy. Finally, validation of IFNAP could only be performed in a comparatively small HCC dataset, as well as cohorts with other cancer types. Therefore, validation of IFNAP in future larger HCC cohorts remains a critical unmet need, particularly in light of the limited number of cases that were used for the construction of the signature.

In summary, our study defines the key molecular drivers of response to anti-PD1 in HCC. We generated and validated a signature recapitulating these pathways that predict response and longer survival in HCC and other cancer types and therefore has potential to maximize the efficiency of anti-PD1 application. The final value of this signature needs to be explored within phase III investigations. In patients treated with second and third line anti-PD1, prior TKI therapy likely impairs the predictive potential of the IFNAP signature, although further studies will be required to clarify the reasons for this observation.

Supplementary Material

Note: To access the supplementary material accompanying this article, visit the online version of *Gastroenterology* at

www.gastrojournal.org, and at http://doi.org/10.1053/j.gastro.2022.09.005.

References

1. Llovet JM, Kelley RK, Villanueva A, et al. Hepatocellular carcinoma. Nat Rev Dis Primers 2021;7:6.
2. Llovet JM, Ricci S, Mazzaferro V, et al. Sorafenib in advanced hepatocellular carcinoma. N Engl J Med 2008; 359:378–390.
3. Kudo M, Finn RS, Qin S, et al. Lenvatinib versus sorafenib in first-line treatment of patients with unresectable hepatocellular carcinoma: a randomised phase 3 non-inferiority trial. Lancet 2018;391:1163–1173.
4. Finn RS, Qin S, Ikeda M, et al. IMbrave150: updated overall survival (OS) data from a global, randomized, open-label phase III study of atezolizumab (atezo) + bevacizumab (bev) versus sorafenib (sor) in patients (pts) with unresectable hepatocellular carcinoma (HCC). J Clin Oncol 2021;39:267.
5. Finn RS, Qin S, Ikeda M, et al. Atezolizumab plus bevacizumab in unresectable hepatocellular carcinoma. N Engl J Med 2020;382:1894–1905.
6. Abou-Alfa Ghassan K, Lau G, Kudo M, et al. Tremelimumab plus durvalumab in unresectable hepatocellular carcinoma. NEJM Evid 2022;1(8); https://doi.org/10.1056/EVIDoa2100070.
7. **Kelley RK, Rimassa L**, Cheng A-L, et al. Cabozantinib plus atezolizumab versus sorafenib for advanced hepatocellular carcinoma (COSMIC-312): a multicentre, open-label, randomised, phase 3 trial. Lancet Oncol 2022; 23:995–1008.
8. Greten TF, Lai CW, Li G, et al. Targeted and immune-based therapies for hepatocellular carcinoma. Gastroenterology 2019;156:510–524.
9. El-Khoueiry AB, Sangro B, Yau T, et al. Nivolumab in patients with advanced hepatocellular carcinoma (CheckMate 040): an open-label, non-comparative, phase 1/2 dose escalation and expansion trial. Lancet 2017;389:2492–2502.
10. Zhu AX, Finn RS, Edeline J, et al. Pembrolizumab in patients with advanced hepatocellular carcinoma previously treated with sorafenib (KEYNOTE-224): a non-randomised, open-label phase 2 trial. Lancet Oncol 2018;19:940–952.
11. Yau T, Park JW, Finn RS, et al. CheckMate 459: a randomized, multi-center phase III study of nivolumab (NIVO) vs sorafenib (SOR) as first-line (1L) treatment in patients (pts) with advanced hepatocellular carcinoma (aHCC). Ann Oncol 2019;30(suppl_5):v851–v934.
12. Finn RS, Ryoo BY, Merle P, et al. Pembrolizumab as second-line therapy in patients with advanced hepatocellular carcinoma in KEYNOTE-240: a randomized, double-blind, phase III trial. J Clin Oncol 2020;38:193–202.
13. Llovet JM, Lencioni R. mRECIST for HCC: performance and novel refinements. J Hepatol 2020;72:288–306.
14. **Isomoto K, Haratani K**, Hayashi H, et al. Impact of EGFR-TKI treatment on the tumor immune microenvironment in EGFR mutation-positive non-small cell lung cancer. Clin Cancer Res 2020;26:2037–2046.
15. Lee H-H, Wang Y-N, Xia W, et al. Removal of N-linked glycosylation enhances PD-L1 detection and predicts anti-PD-1/PD-L1 therapeutic efficacy. Cancer Cell 2019; 36:168–178.e4.
16. **Montironi C, Castet F, Haber PK**, et al. Inflamed and non-inflamed classes of HCC: a revised immunogenomic classification [published online ahead of print February 23, 2022]. Gut http://doi.org/10.1136/gutjnl-2021-325918.
17. Sia D, Jiao Y, Martinez-Quetglas I, et al. Identification of an immune-specific class of hepatocellular carcinoma, based on molecular features. Gastroenterology 2017; 153:812–826.
18. Ayers M, Lunceford J, Nebozhyn M, et al. IFN-γ-related mRNA profile predicts clinical response to PD-1 blockade. J Clin Invest 2017;127:2930–2940.
19. Fehrenbacher L, Spira A, Ballinger M, et al. Atezolizumab versus docetaxel for patients with previously treated non-small-cell lung cancer (POPLAR): a multicentre, open-label, phase 2 randomised controlled trial. Lancet 2016;387:1837–1846.
20. **Sangro B, Melero I**, Wadhawan S, et al. Association of inflammatory biomarkers with clinical outcomes in nivolumab-treated patients with advanced hepatocellular carcinoma. J Hepatol 2020;73:1460–1469.
21. Finkin S, Yuan D, Stein I, et al. Ectopic lymphoid structures function as microniches for tumor progenitor cells in hepatocellular carcinoma. Nat Immunol 2015; 16:1235–1244.
22. Tian S, Roepman P, Popovici V, et al. A robust genomic signature for the detection of colorectal cancer patients with microsatellite instability phenotype and high mutation frequency. J Pathol 2012;228:586–595.
23. **Torrecilla S, Sia D, Harrington AN**, et al. Trunk mutational events present minimal intra- and inter-tumoral heterogeneity in hepatocellular carcinoma. J Hepatol 2017;67:1222–1231.
24. Prat A, Navarro A, Paré L, et al. Immune-related gene expression profiling after PD-1 blockade in non–small cell lung carcinoma, head and neck squamous cell carcinoma, and melanoma. Cancer Res 2017;77:3540–3550.
25. **Jung H, Kim HS**, Kim JY, et al. DNA methylation loss promotes immune evasion of tumours with high mutation and copy number load. Nat Commun 2019;10:4278.
26. **Hugo W, Zaretsky JM**, Sun L, et al. Genomic and transcriptomic features of response to anti-PD-1 therapy in metastatic melanoma. Cell 2016;165:35–44.
27. **Liu D, Schilling B**, Liu D, et al. Integrative molecular and clinical modeling of clinical outcomes to PD1 blockade in patients with metastatic melanoma. Nat Med 2019; 25:1916–1927.
28. Hsu CL, Ou DL, Bai LY, et al. Exploring markers of exhausted CD8 T cells to predict response to immune checkpoint inhibitor therapy for hepatocellular carcinoma. Liver Cancer 2021;10:346–359.
29. Newman AM, Steen CB, Liu CL, et al. Determining cell type abundance and expression from bulk tissues with digital cytometry. Nat Biotechnol 2019;37:773–782.
30. Kamada T, Togashi Y, Tay C, et al. PD-1^{+} regulatory T cells amplified by PD-1 blockade promote hyperprogression of cancer. Proc Natl Acad Sci U S A 2019;116:9999.

31. Ruiz de Galarreta M, Bresnahan E, Molina-Sánchez P, et al. β-Catenin activation promotes immune escape and resistance to anti-PD-1 therapy in hepatocellular carcinoma. Cancer Discov 2019;9:1124–1141.
32. Rooney MS, Shukla SA, Wu CJ, et al. Molecular and genetic properties of tumors associated with local immune cytolytic activity. Cell 2015;160:48–61.
33. Harding JJ, Nandakumar S, Armenia J, et al. Prospective genotyping of hepatocellular carcinoma: clinical implications of next-generation sequencing for matching patients to targeted and immune therapies. Clin Cancer Res 2019;25:2116–2126.
34. von Felden J, Craig AJ, Garcia-Lezana T, et al. Mutations in circulating tumor DNA predict primary resistance to systemic therapies in advanced hepatocellular carcinoma. Oncogene 2021;40:140–151.
35. **Chen P-L, Roh W**, Reuben A, et al. Analysis of immune signatures in longitudinal tumor samples yields insight into biomarkers of response and mechanisms of resistance to immune checkpoint blockade. Cancer Discov 2016;6:827–837.
36. Pfister D, Núñez NG, Pinyol R, et al. NASH limits anti-tumour surveillance in immunotherapy-treated HCC. Nature 2021;592:450–456.
37. **Sade-Feldman M, Jiao YJ**, Chen JH, et al. Resistance to checkpoint blockade therapy through inactivation of antigen presentation. Nat Commun 2017;8:1136.
38. Zhu AX, Abbas AR, de Galarreta MR, et al. Molecular correlates of clinical response and resistance to atezolizumab in combination with bevacizumab in advanced hepatocellular carcinoma. Nat Med 2022;28:1599–1611.
39. Spranger S, Bao R, Gajewski TF. Melanoma-intrinsic β-catenin signalling prevents anti-tumour immunity. Nature 2015;523:231–235.
40. van de Haar J, Hoes LR, Roepman P, et al. Limited evolution of the actionable metastatic cancer genome under therapeutic pressure. Nat Med 2021;27:1553–1563.
41. Torrens L, Montironi C, Puigvehí M, et al. Immunomodulatory effects of lenvatinib plus anti-programmed cell death protein 1 in mice and rationale for patient enrichment in hepatocellular carcinoma. Hepatology 2021;74:2652–2669.
42. Tovar V, Cornella H, Moeini A, et al. Tumour initiating cells and IGF/FGF signalling contribute to sorafenib resistance in hepatocellular carcinoma. Gut 2017;66:530–540.
43. **Ho WJ, Zhu Q**, Durham J, et al. Neoadjuvant cabozantinib and nivolumab converts locally advanced HCC into resectable disease with enhanced antitumor immunity. Nat Cancer 2021;2:891–903.

Author names in bold designate shared co-first authorship.

Received June 7, 2021. Accepted September 2, 2022.

Correspondence
Address correspondence to: Josep M. Llovet, MD, PhD, Mount Sinai Liver Cancer Program, Division of Liver Diseases, Tisch Cancer Institute, Icahn School of Medicine at Mount Sinai, Madison Avenue 1425, New York, New York 10029. e-mail: josep.llovet@mssm.edu.

CRediT Authorship Contributions
Order of Authors (with Contributor Roles):

Philipp K. Haber, MD (Conceptualization: Lead; Data curation: Lead; Formal analysis: Lead; Investigation: Lead; Methodology: Lead; Writing – original draft: Lead).

Florian Castet, MD (Formal analysis: Supporting; Investigation: Supporting; Methodology: Supporting; Writing – original draft: Supporting).

Miguel Torres-Martín, PhD (Data curation: Equal; Formal analysis: Equal; Methodology: Supporting).

Carmen Andreu-Oller, MSc (Data curation: Supporting; Formal analysis: Supporting; Writing – review & editing: Supporting).

Marc Puigvehí, MD, PhD (Conceptualization: Supporting; Data curation: Supporting; Formal analysis: Supporting; Methodology: Supporting; Writing – review & editing: Supporting).

Miho Maeda, MSc (Data curation: Supporting; Methodology: Supporting).

Pompilia Radu, MD, PhD (Investigation: Supporting; Methodology: Supporting).

Jean-François Dufour, MD (Investigation: Supporting; Methodology: Supporting).

Chris Verslype, MD, PhD (Investigation: Supporting; Methodology: Supporting).

Carolin Zimpel, MD (Investigation: Supporting; Methodology: Supporting).

Jens U. Marquardt, MD, PhD (Investigation: Supporting; Methodology: Supporting).

Peter R. Galle, MD, PhD (Investigation: Supporting; Methodology: Supporting).

Arndt Vogel, MD, PhD (Investigation: Supporting; Methodology: Supporting).

Melanie Bathon, MD (Investigation: Supporting; Methodology: Supporting).

Tim Meyer, MD, PhD (Investigation: Supporting; Methodology: Supporting).

Ismail Labgaa, MD, PhD (Investigation: Supporting; Methodology: Supporting).

Antonia Digklia, MD (Investigation: Supporting; Methodology: Supporting).

Lewis R. Roberts, MD, PhD (Investigation: Supporting; Methodology: Supporting).

Mohamed A. Mohamed Ali, MD (Investigation: Supporting; Methodology: Supporting).

Beatriz Mínguez, MD, PhD (Investigation: Supporting; Methodology: Supporting).

Davide Citterio, MD (Investigation: Supporting; Methodology: Supporting).

Vincenzo Mazzaferro, MD, PhD (Investigation: Supporting; Methodology: Supporting).

Fabian Finkelmeier, MD (Investigation: Supporting; Methodology: Supporting).

Jörg Trojan, MD, PhD (Investigation: Supporting; Methodology: Supporting).

Burcin Özdirik, MD (Investigation: Supporting; Methodology: Supporting).

Tobias Müller, MD (Investigation: Supporting; Methodology: Supporting).

Moritz Schmelzle, MD (Investigation: Supporting; Methodology: Supporting).

Anthony Bejjani, MD (Investigation: Supporting; Methodology: Supporting).

Max W. Sung, MD (Investigation: Supporting; Methodology: Supporting).

Myron E. Schwartz, MD (Investigation: Supporting; Methodology: Supporting).

Richard S. Finn, MD (Investigation: Supporting; Methodology: Supporting).

Swan Thung, MD (Investigation: Supporting; Methodology: Supporting).

Augusto Villanueva, MD, PhD (Investigation: Supporting; Methodology: Supporting).

Daniela Sia, PhD (Investigation: Supporting; Methodology: Supporting).

Josep M. Llovet, MD, PhD (Funding acquisition: Lead; Investigation: Lead; Methodology: Lead; Writing – original draft: Lead; Writing – review & editing: Lead).

Conflicts of Interest
These authors disclose the following: Jean-Francois Dufour has received consulting fees from AbbVie, Bayer Healthcare, Bristol-Myers Squibb, Falk, Genfit, Genkyotex, Gilead Sciences, HepaRegenix, Intercept, Eli Lilly, Merck, Novartis, Roche. Jens U. Marquardt received honoraria from Roche, Bayer, Ipsen, Merz, AstraZeneca, MSD, and Leap-Tx, Eisai. Peter R. Galle is receiving honoraria from Adaptimmune, Bayer, BMS, AstraZeneca, Sirtex, MSD, Eisai, Ipsen, Roche, Lilly, and Guerbet. Arndt Vogel has received consulting fees and honoraria from AstraZeneca, Bayer, BMS, Eisai, Incyte, Ipsen, Janssen, Lilly, Merck, MSD, Novartis, Pierre Fabre, Roche, and Sanofi. Tim Meyer reports consulting fees from Ipsen, AstraZeneca, Roche, Bayer Healthcare, Adaptimmune, Boston Scientific, and Eisai. Lewis R. Roberts has received grant funding from Bayer, BTG International, Exact Sciences, Gilead Sciences, GlycoTest, Redhill, TARGET PharmaSolutions, and FUJIFILM Medical Systems, and has consulted for AstraZeneca, Bayer, Exact Sciences, Gilead Sciences, GRAIL, QED Therapeutics, and TAVEC. Beatriz Mínguez received consultancy fees from Bayer-Shering Pharma and Eisai-Merck, lectures/speaker fees from Eisai, MSD, and Roche, and a research grant from Laboratorios Viñas S.L. Moritz Schmelzle is receiving honoraria from ERBE, Amgen, Merck, and Bayer Healthcare. Max W. Sung is receiving consulting fees from Bayer, EISAI, and Exelixis. Richard S. Finn has received consulting fees from AstraZeneca, Bayer Healthcare, Eisai, CStone, Bristol-Myers Squibb, Eli Lilly, Pfizer, Merck, Roche/Genenetech, and Exelixis. Augusto Villanueva has received consulting fees from Guidepoint, Fujifilm, Boehringer Ingelheim, FirstWord, and MHLife. Josep M. Llovet is receiving research support from Bayer HealthCare Pharmaceuticals, Eisai Inc, Bristol-Myers Squibb, Boehringer Ingelheim, and Ipsen, and consulting fees from Eli

Lilly, Bayer HealthCare Pharmaceuticals, Bristol-Myers Squibb, Eisai Inc, Celsion Corporation, Exelixis, Merck, Ipsen, Genentech, Roche, Glycotest, Nucleix, Sirtex, Mina Alpha Ltd and AstraZeneca. The remaining authors disclose no conflicts.

Funding

This study was supported by a research grant from Bayer Pharmaceuticals to Josep M. Llovet. Philipp K. Haber is supported by the fellowship grant of the German Research Foundation (DFG, HA 8754/1–1). Florian Castet is supported by an AECC Clínico Junior grant, ID code (CLJUN20007CAST). Carmen Andreu-Oller is supported by a Fulbright fellowship. Marc Puigvehí received a "Juan Rodés" scholarship grant from Asociación Española para el Estudio del Hígado (AEEH). Jens U. Marquardt is supported by grants from the German Research Foundation (MA 4443/2–2; SFB1292) and the Volkswagen Foundation (Lichtenberg program). Arndt Vogel is funded by the DFG (SFB/TRR 209 - 314905040, and Vo959/9–1). Tim Meyer is funded by the NIHR UCH Biomedical Research Centre and Accelerator Award (HUNTER, Ref. C9380/A26813, partnership between the CRUK, AECC, and AIRC). Lewis R. Roberts and Mohamed A. Mohamed Ali are supported by the Mayo Clinic Hepatobiliary SPORE (P50 CA210964). Beatriz Mínguez is funded by Instituto de Salud Carlos III (ISCIII) (PI18/00961 and PI21/00714 co-funded by European Union). Moritz Schmelzle acknowledges a research grant from the DFG (SCHM2661/3–2). The work of Daniela Sia is supported by the Tisch Cancer Institute and the PhD Scientist Innovative Research Award. Josep M. Llovet is supported by National Cancer Institute (P30-CA196521), National Institute of Diabetes and Digestive and Kidney Diseases (R01 DK128289), US Department of Defense (CA150272P3), European Commission/Horizon 2020 Program (HEPCAR, Ref. 667273–2), Accelerator Award (CRUK, AECC, AIRC) (HUNTER, Ref. C9380/A26813), Samuel Waxman Cancer Research Foundation, Centro de Investigación Biomédica en Red (CIBER) – ISCIII, Spanish National Health Institute (SAF2016–76390), Generalitat de Catalunya/AGAUR (SGR-1358), and the Acadèmia de Ciències Mèdiques i de la Salut de Catalunya i de Balears.

Supplementary Materials and Methods

Study Population and Endpoints

Gene expression profiles from 347 patients undergoing anti-PD1 therapy were analyzed for the purpose of our study, including our HCC cohort of 83 cases established under the umbrella of an international consortium comprising 13 referral centers. Cases from our cohort were recruited from the following institutions: Icahn School of Medicine at Mount Sinai, the Inselspital University of Bern, KU Leuven, University of Mainz, Hannover Medical School, University College London Cancer Institute, Lausanne University Hospital, Mayo Clinic, Hospital Universitari Vall d'Hebron, IRCCS Istituto Nazionale Tumori (Milan, Italy), University of Frankfurt, Charité University Medicine Berlin, and the Geffen School of Medicine at UCLA. The transcriptomic data from the remaining 240 cases were previously published and obtained from public repositories.[1–4] Clinico-pathologic data and follow-up for patients included in the internal cohort of 83 patients are summarized in Table 1 and Supplementary Tables 2 and 3.

RNA Extraction and Gene Expression Profiling

We collected 111 archived formalin-fixed paraffin-embedded (FFPE) tissue blocks (Supplementary Table 1), including both resection specimen and biopsies, of patients undergoing anti-PD1 therapy for aHCC. The study protocol was approved at each contributing center and informed consent obtained from subjects. An expert liver pathologist (S.T.) validated HCC as the disease entity and discerned tumor tissue from adjacent nontumoral hepatic parenchyma based on haematoxylin-eosin staining. Briefly, tumor tissue was macrodissected in FFPE sections and RNA as well as genomic DNA isolated using the miRNAeasy FFPE and QIAmp DNA FFPE tissue kit (QIAgen, Hilden, Germany), respectively.

Transcriptomic studies were performed using the Clariom S human Array (Affymetrix, Santa Clara, CA) with 400 ng of total RNA as input. We performed the microarrays in 2 different batches of 58 samples and 29 cases, respectively. The latter batch included 4 technical replicates from the first batch to allow for subsequent batch correction, if necessary. Nonetheless, after applying an empirical Bayes framework with ComBat—integrated in sva bioconductor package[5]—no differences were observed between batches, and therefore technical replicates were removed from the first set. Commands mod=NULL, and par.prior=TRUE were used in ComBat. Background correction and quantile normalization of the raw expression data was carried out using the R *oligo* package with *rma* modules. Differential gene expression based on the distinct response subtypes was conducted using the *limma* package. We performed Wilcoxon rank-sum test on an individual gene level and used a nominal P value threshold <0.01 and a fold change (FC) of 1.5 as cutoffs to define differentially expressed genes. Functional characterization of differentially expressed genes was performed using Gene Ontology enrichment analysis with false discovery rate (FDR) corrected P values. We further tested previously reported gene expression signatures that define states of inflammation and immune cell subsets using the Molecular Signature Database gene sets (MSigDB, www.broadinstitute.org/msigdb) and individually curated gene sets[6–13] (signatures are shown in Supplementary Table 6). This included signatures that have been previously linked to response to immunotherapy in HCC and other cancer types. Gene sets with an upregulation of all included genes were tested via single sample gene set enrichment analysis (GSEA) after normalization. Assessment of pathway activation was performed using GSEA and single sample GSEA. Other signatures that incorporate up- and downregulation of genes as well as previously reported molecular HCC classes[11,14,15] were tested using the GenePattern Nearest Template Prediction module.[16] Samples were assigned to a given class when the FDR <0.05 unless otherwise stated in the original publication. Microenvironmental deconvolution was performed with CIBERSORTx[17] in batch corrected mode.

Generation of the IFNAP Signature

To generate a gene expression signature associated with objective response to anti-PD1 single-agent therapy, differential expression analysis was performed between responders and nonresponders, and genes with an FC >1.5 and a P value by Wilcoxon rank-sum test of $<.01$ selected for further analysis. The resulting 140 genes were able to distinguish responding from nonresponding cases based on principal component analysis (Supplementary Figure 2*A*). We next cross-referenced the 140 genes with the 2 top Gene Ontology (GO) terms associated with these genes pertaining to IFN signaling (GO:0060333) and antigen presentation (GO:0019886). We added *CXCL9* (FC $= 3.4$, $P < .01$) and *B2M* (FC $= 1.7$, $P = .01$) that were enriched in responders in our dataset as well. *CXCL9* is a key chemokine, facilitating tumoral T-cell infiltration that has been shown in a recent metaanalysis to be significantly enriched among responding patients across cancer types.[18] *B2M* is a part of the antigen-presentation machinery, in which loss of heterozygosity and deletions have been linked to primary resistance in melanoma.[19] The resulting 11 genes were incorporated into a gene set titled IFNAP that was then tested to predict response and survival in our HCC cohort and 4 validation datasets. We defined high expression of IFNAP as patients within the third tertile, whereas the remaining patients were characterized as the Rest. A summary of the generation of the signature is depicted in Supplementary Figure 13.

Validation of IFNAP in External Datasets

After ensuring acceptable predictive ability in our dataset, we then sought to test the predictive potential of IFNAP in 5 independent external datasets that were previously published:

1. Prat et al, Cancer Res 2017: 65 patients (melanoma, non–small-cell lung cancer [NSCLC], head and neck squamous cell carcinoma)[3]
2. Jung et al, Nat Comm 2019: 27 patients (NSCLC)[1]
3. Liu et al, Nat Med. 2019: 151 patients (melanoma)[2]

4. Hugo et al, Cell 2016: 28 patients (melanoma)[4]
5. Hsu et al, Liver Cancer 2021: 24 patients (HCC)[20]

As in our internal cohort, IFNAP expression was defined as high for the top tertile, whereas the remaining patients were grouped as the Rest in each of the datasets. In the cohort by Jung et al,[1] response was defined as patients having a durable clinical benefit, meaning the patient had either OR SD for at least 6 months.

In all datasets, tissue was obtained before the initiation of anti-PD1 therapy. In the Liu et al cohort,[2] however, 1 patient had an on-treatment biopsy. This patient was therefore excluded from the analysis.

In both pure melanoma datasets, response rates exceeded 33% and therefore the applied cutoff for the third tertile limited the predictive ability of IFNAP. In these datasets, χ^2 *P* values are 1-sided.

The effect of TKIs on tumoral and microenvironmental signaling was studied by repurposing a previously published report in which a syngeneic HCC model was generated by injecting 5×10^6 Hepa1-6 cells in 5- to 6-week-old female C57BL/6J mice.[21] Tumor samples from the model were collected 13 days after treatment with either lenvatinib or vehicle and subjected to gene expression microarray studies using the Clariom S Mouse Array (Affymetrix; GSE153203). Normalization, background correction, and log-transformation were carried out using the limma package and single sample GSEA performed using GenePattern.

Immunohistochemistry and Assessment of Immune Infiltration

The presence and severity of an immune infiltrate was assessed by an expert pathologist (ST) using hematoxylin-eosin–stained slides. A previously published scoring system was applied grading the overall amount of the immune infiltrate applying a semi-quantitative score from 0 to 4, where 0 = absence of immune cell infiltration, 1 = minimal, 2 = mild infiltration, 3 = moderate infiltration, and 4 = severe infiltration.[11] We applied the previously established threshold of 2, up to which samples are defined to have low infiltration where grades 3 and 4 are considered to have high infiltration. Scoring was performed both within the tumoral compartment as well as at the invasive margin when available.

Assessment of the tumor infiltration lymphocytes (TILs) and scoring was performed following the International Immuno-Oncology Biomarkers Working Group recommendations.[22]

Immunohistochemistry for PD1 and PD-L1 was performed on 3-μm-thick FFPE tissue sections after heat-induced antigen retrieval in a microwave with 10 mM TRIS-EDTA (pH = 9). Primary antibodies used for anti-PD-L1 and anti-PD1 were Abcam clone 28-8 and clone NAT105, respectively. Positive staining for PD1 was measured as previously characterized using a semi-quantitative (high vs low) score.[11] PD-L1 expression was assessed in HCC cells in which the percentage of neoplastic cells with membranous staining was defined and tumors with 1% or more of positively stained cells were classified as positive.

CTNNB1 Mutation Status

As mutations in *CTNNB1* have been implicated in driving primary resistance to anti-PD1 therapy, we performed Sanger sequencing using primers to amplify *CTNNB1* exon 3. Mutations were confirmed by sequencing a second amplification product on both strands. Primers used were 5′ to 3′ GATTTGATGGAGTTGGACATGG (forward) and TGTTCTTGAGTGAAGGACTGAG (reverse).

Statistical Analysis

Supplementary analyses were performed using the R statistical package. Correlations between expression of gene signatures and objective response were performed by χ^2 test and Wilcoxon rank-sum test for categorical and continuous data, respectively. Kaplan-Meier estimates and log-rank test were performed to investigate the association of IFNAP expression with PFS and OS using the *survminer* package.

Molecular Data Availability

Publically available datasets used in this study are detailed in the "Validation of IFNAP in External Datasets" section in the Supplementary Materials and Methods. The normalized gene expression data and clinical data from the HCC cohort has been deposited at European Genome archive (EGAS00001005477). All reasonable requests for raw data will be promptly reviewed by the corresponding author to determine whether the request is subject to any intellectual property or confidentiality obligations.

References

1. Jung H, Kim HS, Kim JY, et al. DNA methylation loss promotes immune evasion of tumours with high mutation and copy number load. Nat Commun 2019;10:4278.
2. Liu D, Schilling B, Liu D, et al. Integrative molecular and clinical modeling of clinical outcomes to PD1 blockade in patients with metastatic melanoma. Nat Med 2019; 25:1916–1927.
3. Prat A, Navarro A, Paré L, et al. Immune-related gene expression profiling after PD-1 blockade in non–small cell lung carcinoma, head and neck squamous cell carcinoma, and melanoma. Cancer Res 2017; 77:3540–3550.
4. Hugo W, Zaretsky JM, Sun L, et al. Genomic and transcriptomic features of response to anti-PD-1 therapy in metastatic melanoma. Cell 2016;165:35–44.
5. Leek JT, Johnson WE, Parker HS, et al. The sva package for removing batch effects and other unwanted variation in high-throughput experiments. Bioinformatics 2012; 28:882–883.
6. Ayers M, Lunceford J, Nebozhyn M, et al. IFN-γ-related mRNA profile predicts clinical response to PD-1 blockade. J Clin Invest 2017;127:2930–2940.

7. Rooney MS, Shukla SA, Wu CJ, et al. Molecular and genetic properties of tumors associated with local immune cytolytic activity. Cell 2015;160:48–61.
8. Sangro B, Melero I, Wadhawan S, et al. Association of inflammatory biomarkers with clinical outcomes in nivolumab-treated patients with advanced hepatocellular carcinoma. J Hepatol 2020;73:1460–1469.
9. Auslander N, Zhang G, Lee JS, et al. Robust prediction of response to immune checkpoint blockade therapy in metastatic melanoma. Nat Med 2018;24:1545–1549.
10. Fehrenbacher L, Spira A, Ballinger M, et al. Atezolizumab versus docetaxel for patients with previously treated non-small-cell lung cancer (POPLAR): a multicentre, open-label, phase 2 randomised controlled trial. Lancet 2016;387:1837–1846.
11. Sia D, Jiao Y, Martinez-Quetglas I, et al. Identification of an Immune-specific class of hepatocellular carcinoma, based on molecular features. Gastroenterology 2017; 153:812–826.
12. Pinyol R, Montal R, Bassaganyas L, et al. Molecular predictors of prevention of recurrence in HCC with sorafenib as adjuvant treatment and prognostic factors in the phase 3 STORM trial. Gut 2019;68:1065–1075.
13. Bindea G, Mlecnik B, Tosolini M, et al. Spatiotemporal dynamics of intratumoral immune cells reveal the immune landscape in human cancer. Immunity 2013; 39:782–795.
14. Hoshida Y, Nijman SM, Kobayashi M, et al. Integrative transcriptome analysis reveals common molecular subclasses of human hepatocellular carcinoma. Cancer Res 2009;69:7385–7392.
15. Chiang DY, Villanueva A, Hoshida Y, et al. Focal gains of VEGFA and molecular classification of hepatocellular carcinoma. Cancer Res 2008;68:6779–6788.
16. Brunet J-P, Tamayo P, Golub TR, et al. Metagenes and molecular pattern discovery using matrix factorization. Proc Natl Acad Sci U S A 2004;101:4164.
17. Newman AM, Steen CB, Liu CL, et al. Determining cell type abundance and expression from bulk tissues with digital cytometry. Nat Biotechnol 2019; 37:773–782.
18. Litchfield K, Reading JL, Puttick C, et al. Meta-analysis of tumor- and T cell-intrinsic mechanisms of sensitization to checkpoint inhibition. Cell 2021;184:596–614.e14.
19. Sade-Feldman M, Jiao YJ, Chen JH, et al. Resistance to checkpoint blockade therapy through inactivation of antigen presentation. Nat Commun 2017;8:1136.
20. Hsu CL, Ou DL, Bai LY, et al. Exploring markers of exhausted CD8 T cells to predict response to immune checkpoint inhibitor therapy for hepatocellular carcinoma. Liver Cancer 2021;10:346–359.
21. Torrens L, Montironi C, Puigvehí M, et al. Immunomodulatory effects of lenvatinib plus anti-programmed cell death protein 1 in mice and rationale for patient enrichment in hepatocellular carcinoma. Hepatology 2021; 74:2652–2669.
22. Hendry S, Salgado R, Gevaert T, et al. Assessing tumor-infiltrating lymphocytes in solid tumors: a practical review for pathologists and proposal for a standardized method from the International Immuno-Oncology Biomarkers Working Group: Part 2: TILs in melanoma, gastrointestinal tract carcinomas, non-small cell lung carcinoma and mesothelioma, endometrial and ovarian carcinomas, squamous cell carcinoma of the head and neck, genitourinary carcinomas, and primary brain tumors. Adv Anat Pathol 2017; 24:311–335.

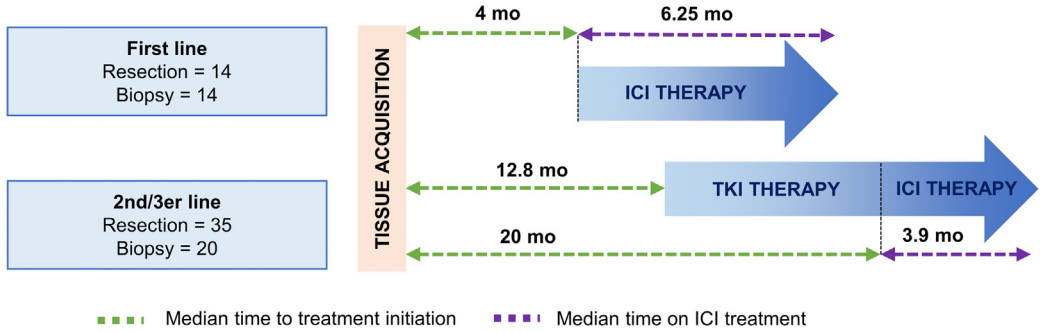

Supplementary Figure 1. Depiction showing the time between sample acquisition and treatment initiation. The time difference between the acquisition of the biological specimen and the initiation of systemic therapies was 4 months in patients treated with anti-PD1 in frontline and 12.8 months for patients treated in second or third line.

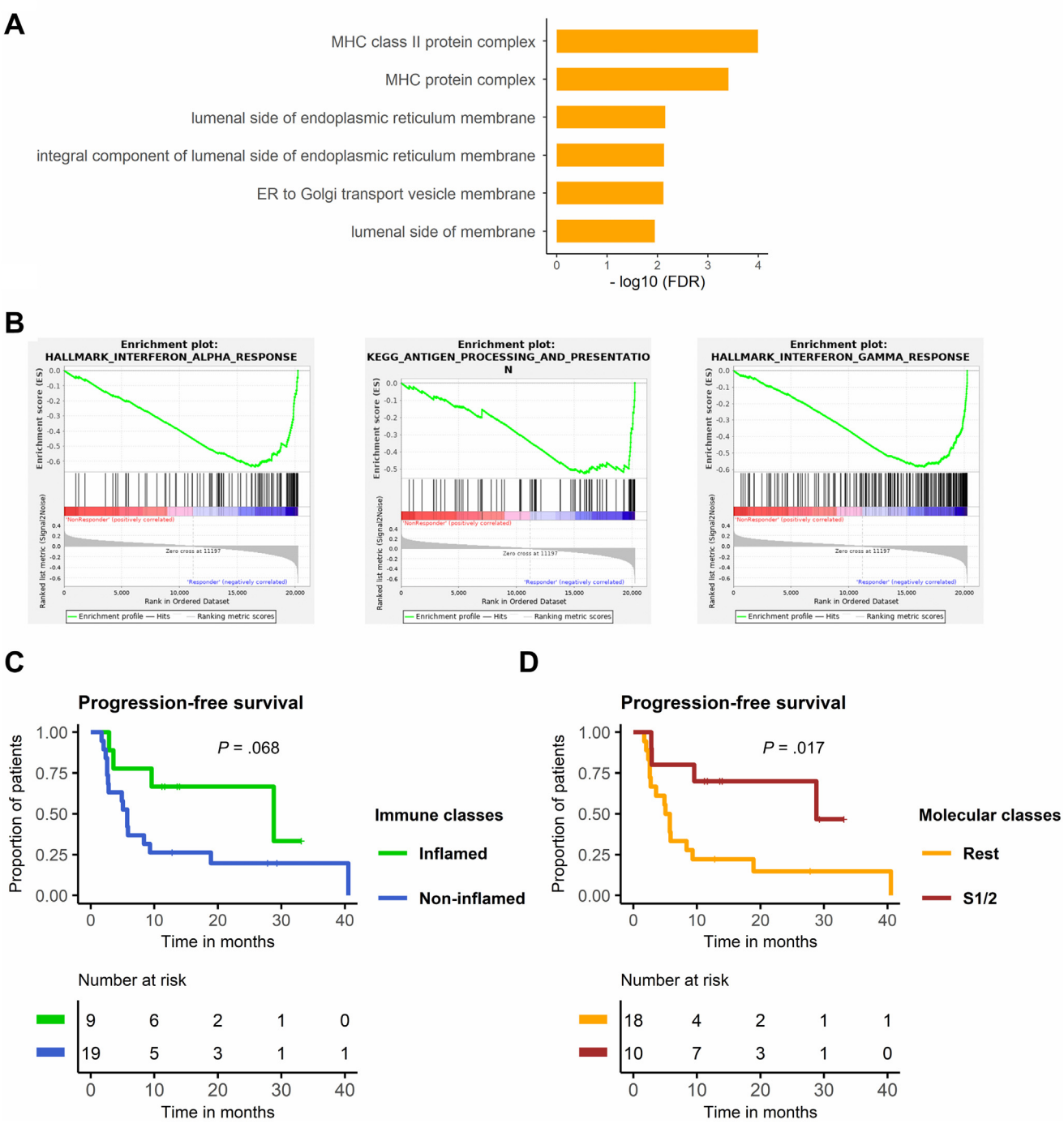

Supplementary Figure 2. Pathway activation in responding patients and clinical outcomes according to the HCC molecular classes. (*A*) GO-term analysis for cellular components among the 140 differentially expressed genes revealed a strong association enrichment in genes associated with MHC class II expression and formation (FDR <0.001). (*B*) Gene set enrichment analysis (GSEA) between responding patients treated with anti-PD1 in frontline (n = 12) compared with nonresponders (n = 16) confirmed an upregulation of genesets associated with an active immune response and antigen presentation (FDR <0.001). (*C*) Outcome analysis in patients treated with anti-PD1 in frontline revealed a trend toward longer PFS in the *Inflamed HCC* subclass was observed. (*D*) Patients with an aggressive phenotype, as accounted for by the molecular classes *S1* and *S2* had a markedly longer PFS than the remaining patients.

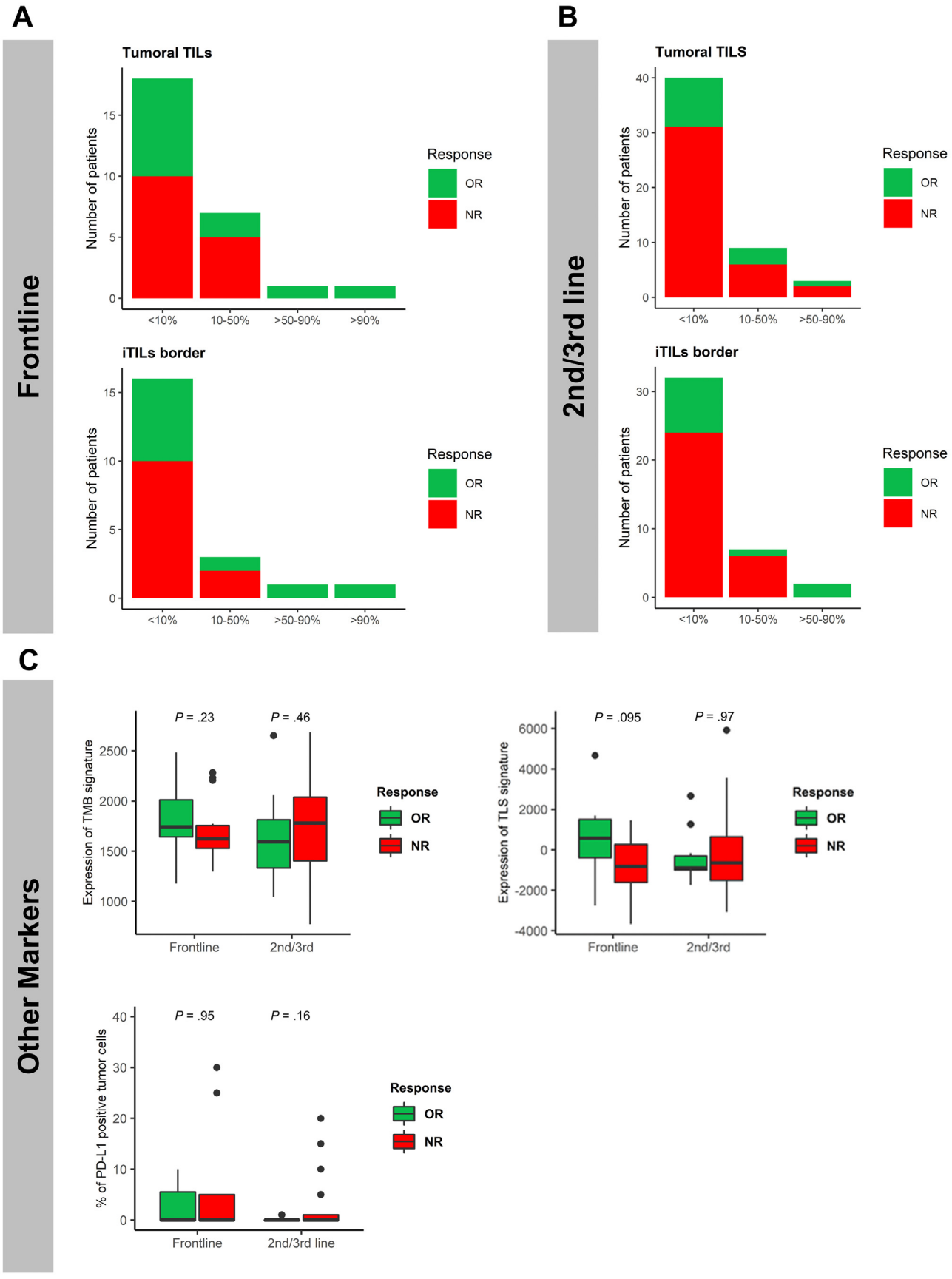
A
Frontline
Tumoral TILs
Number of patients
<10%
10-50%
>50-90%
>90%
Response
OR
NR
iTILs border
B
2nd/3rd line
Tumoral TILS
C
Other Markers
P = .23
P = .46
Expression of TMB signature
Frontline
2nd/3rd
P = .095
P = .97
Expression of TLS signature
P = .95
P = .16
% of PD-L1 positive tumor cells
2nd/3rd line

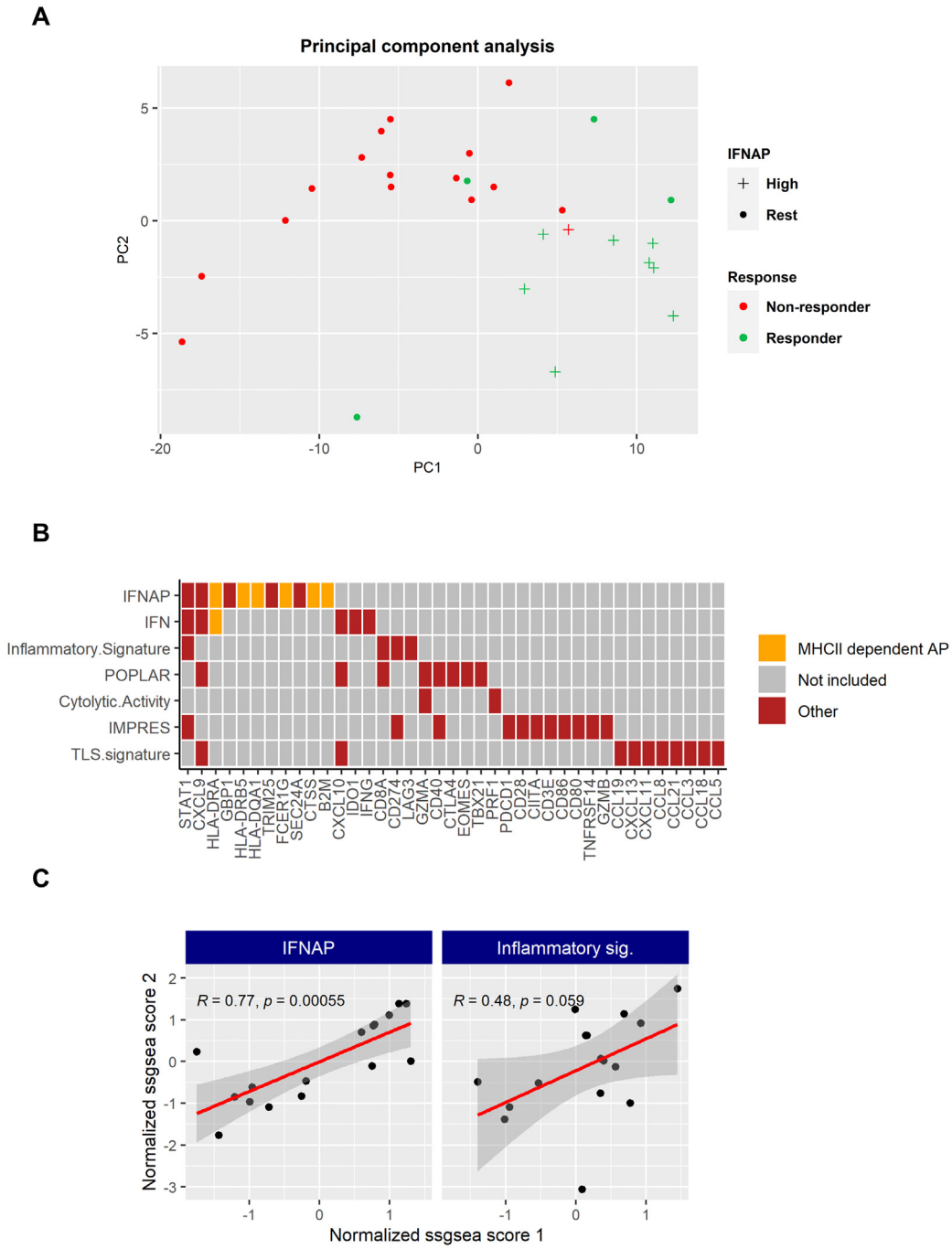

Supplementary Figure 4. Principal component analysis and composition of IFNAP and other signatures. (*A*) Principal component analysis using the 140 differentially expressed genes reveals a clear separation between responding and non-responding patients, with IFNAP-positive patients clustering together. (*B*) Individual compositions of gene expression signatures previously reported and IFNAP are shown highlighting the unique composition of IFNAP. *Red squares* indicate the inclusion of an individual gene in the respective signature. (*C*) Re-analysis of a previously published cohort of 30 samples from 15 large HCC tumors revealed expression of IFNAP to be highly correlated between 2 samples of a given tumor indicating that intratumoral heterogeneity does not mitigate the robustness of the signature.

Supplementary Figure 3. Performance of histologic markers and inferred tumor mutational burden (TMB) in patients treated with anti-PD1 frontline and second/third line. (*A*) No difference was observed between responders and nonresponders treated in frontline based on histologic assessment of tumor infiltrating lymphocytes (TILs) within the tumor (*top*) or at the invasive margin (*bottom*). (*B*) In patients treated in second and third line, a similar observation was made, where the severity of TIL infiltration was not linked to response. (*C*) Expression of previously reported signatures inferring high mutational burden (TMB) and the presence of tertiary lymphoid structures (TLS) was not linked to response status in frontline or in second/third line.

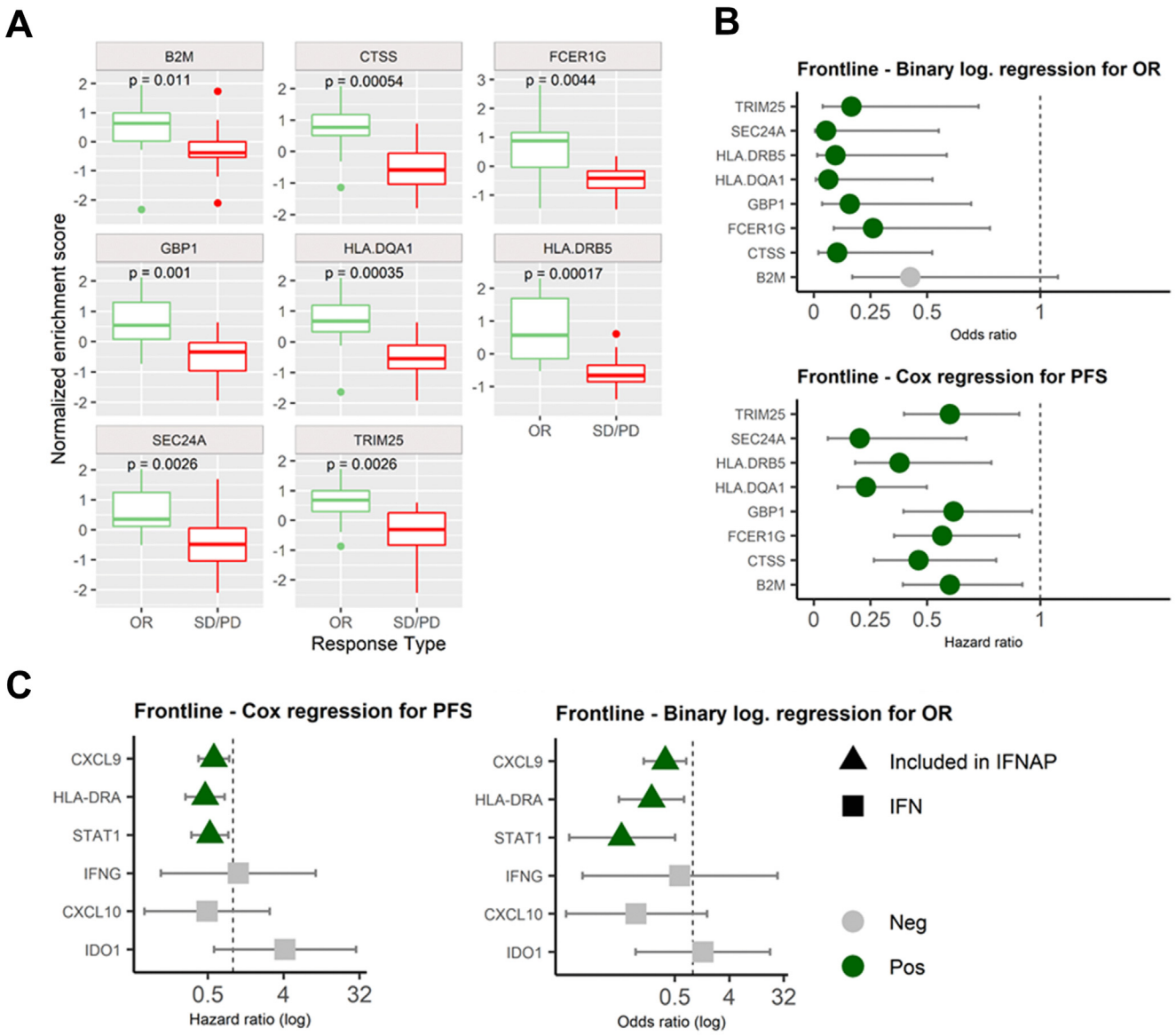

Supplementary Figure 5. Association of outcomes and individual genes in response signatures. Analysis of the genes included in the IFNAP and IFN signature revealed a significant enrichment of all individual IFNAP genes in responders (*A*). Superior clinical outcomes were observed with regard to OR when performing binary logistic regression and to PFS with Cox regression analysis (*B*). Of the 6 genes included in the IFN signature only the ones overlapping with IFNAP were positively linked with OR and longer PFS, whereas the remaining 3 genes (IFNG, CXCL10, and IDO1) were not (*C*).

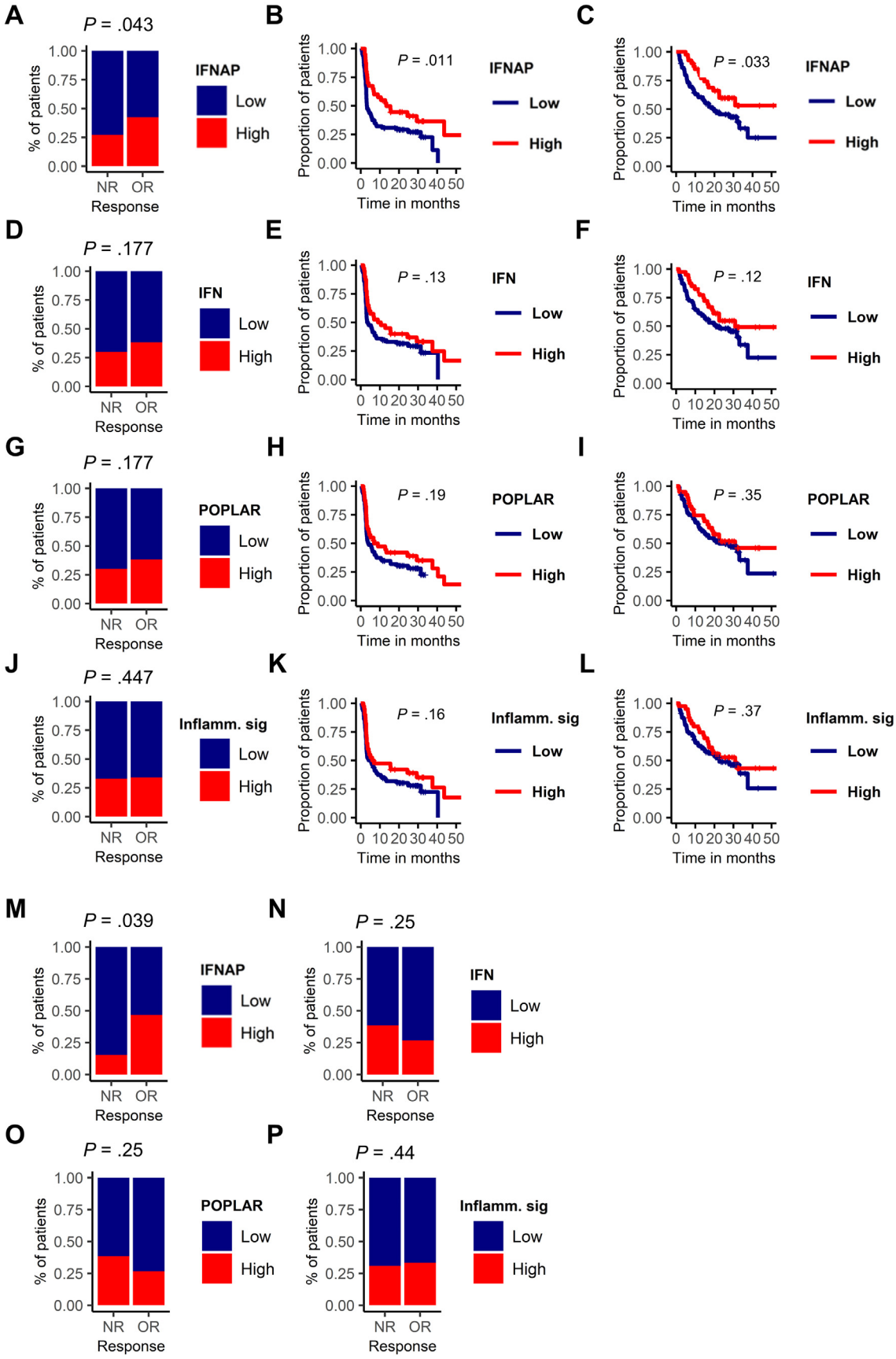
A
P = .043
% of patients
1.00
0.75
0.50
0.25
0.00
NR OR
Response
IFNAP
Low
High
B
P = .011
Proportion of patients
0 10 20 30 40 50
Time in months
IFNAP
Low
High
C
P = .033
Proportion of patients
Time in months
IFNAP
Low
High
D
P = .177
% of patients
Response
IFN
Low
High
E
P = .13
Proportion of patients
Time in months
IFN
Low
High
F
P = .12
Proportion of patients
Time in months
IFN
Low
High
G
P = .177
% of patients
Response
POPLAR
Low
High
H
P = .19
Proportion of patients
Time in months
POPLAR
Low
High
I
P = .35
Proportion of patients
Time in months
POPLAR
Low
High
J
P = .447
% of patients
Response
Inflamm. sig
Low
High
K
P = .16
Proportion of patients
Time in months
Inflamm. sig
Low
High
L
P = .37
Proportion of patients
Time in months
Inflamm. sig
Low
High
M
P = .039
% of patients
Response
IFNAP
Low
High
N
P = .25
% of patients
Response
IFN
Low
High
O
P = .25
% of patients
Response
POPLAR
Low
High
P
P = .44
% of patients
Response
Inflamm. sig
Low
High

Supplementary Figure 6. Validation of IFNAP in 2 independent melanoma cohorts. Correlations between response signature expression, according to the top tertile vs remaining cases, and ORRs as well as Kaplan-Meier estimates for PFS and OS are shown. (*A*–*L*) In a third dataset, including only melanoma cases treated with anti-PD1, only IFNAP was able to consistently show significant differences in terms of OR (*A*), PFS (*B*), and OS (*C*). Conversely, none of the previously reported response signatures (*D*–*L*) were able to elicit significant differences in terms of OR (*D*, *G*, *J*), PFS (*E*, *H*, *K*), and OS (*C*, *F*, *I*, *L*). (*M*–*P*) Validation was performed in a further RNA-sequencing based dataset of patients with melanoma treated with anti-PD1.[4] Of the tested signatures, only high expression of IFNAP was associated with an increase in ORR (*M*), whereas neither the 6-gene *IFN* signature, nor *POPLAR* and the *Inflammatory* signature predicted response (*N*–*P*). No data on PFS were available in this dataset. *P* values in χ^2 tests represent a 1-sided significance level.

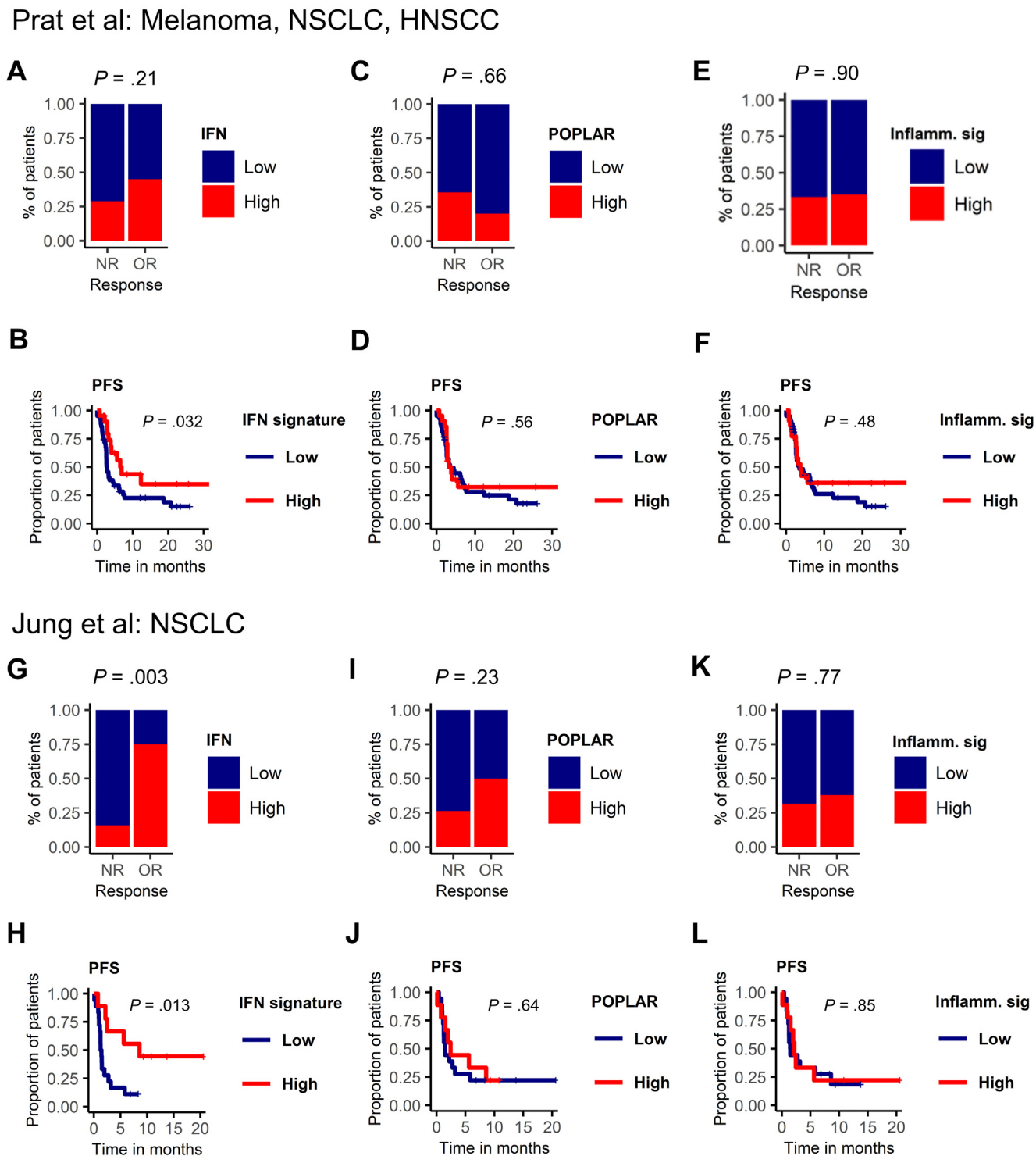

Supplementary Figure 7. Performance of previously reported response signatures in 2 validation datasets. Correlations between response signature expression, according to the top tertile vs remaining cases, and ORRs as well as Kaplan-Meier estimates for PFS are shown. (*A–F*) In the nanostring-based datasets with patients with non–small-cell lung cancer (NSCLC), melanoma, or head and neck squamous cell cancer, none of the previously reported signatures were associated with response (*A*, *C*, *E*), whereas high expression of the IFN signature was associated with longer PFS (*B*). (*G–L*) In the RNA-sequencing based dataset by Jung et al,[1] comprising patients with NSCLC, only IFNAP and the IFN signature was associated with response (*G*) and longer PFS (*H*), whereas the remaining signatures had no predictive values (*I–L*). A cutoff at between the second and third expression tertile was applied to separate the groups. *P* values in χ^2 tests represent a 2-sided significance level.

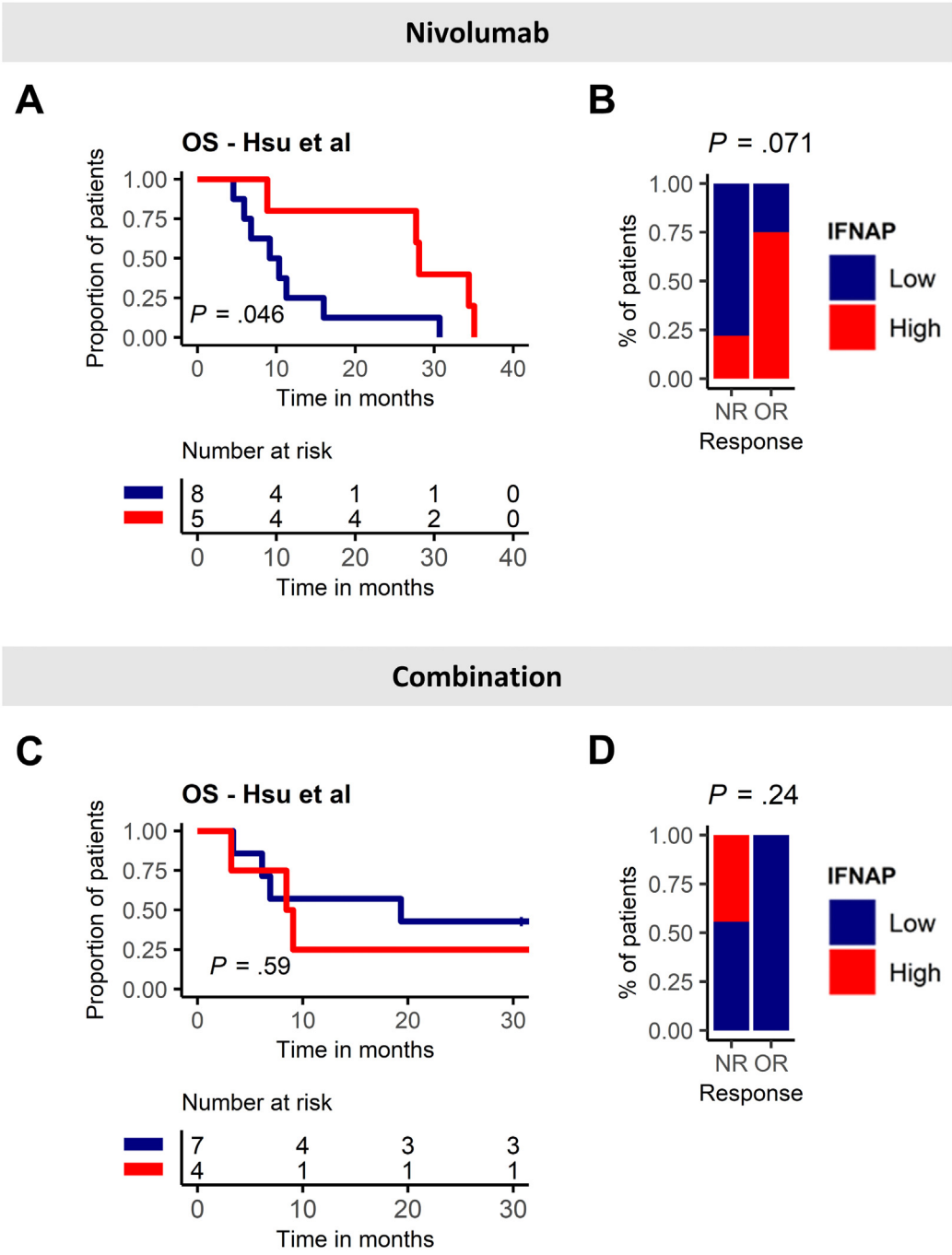

Supplementary Figure 8. Validation of IFNAP in independent HCC cohort. Validation was performed in an independent cohort of 24 patients with HCC treated with either nivolumab (n = 13) or combination (n = 11). Among the patients treated with nivolumab, high expression of IFNAP was associated with significantly longer OS (*A*), whereas a trend was observed toward higher ORR in patients with high IFNAP expression (*B*). In those patients treated with combination, however, high IFNAP expression was neither associated with neither OS (*C*) nor OR (*D*). *P* values represent log-rank test in Kaplan-Meier curves as well as asymptotic χ^2 tests with a 2-sided significance level.

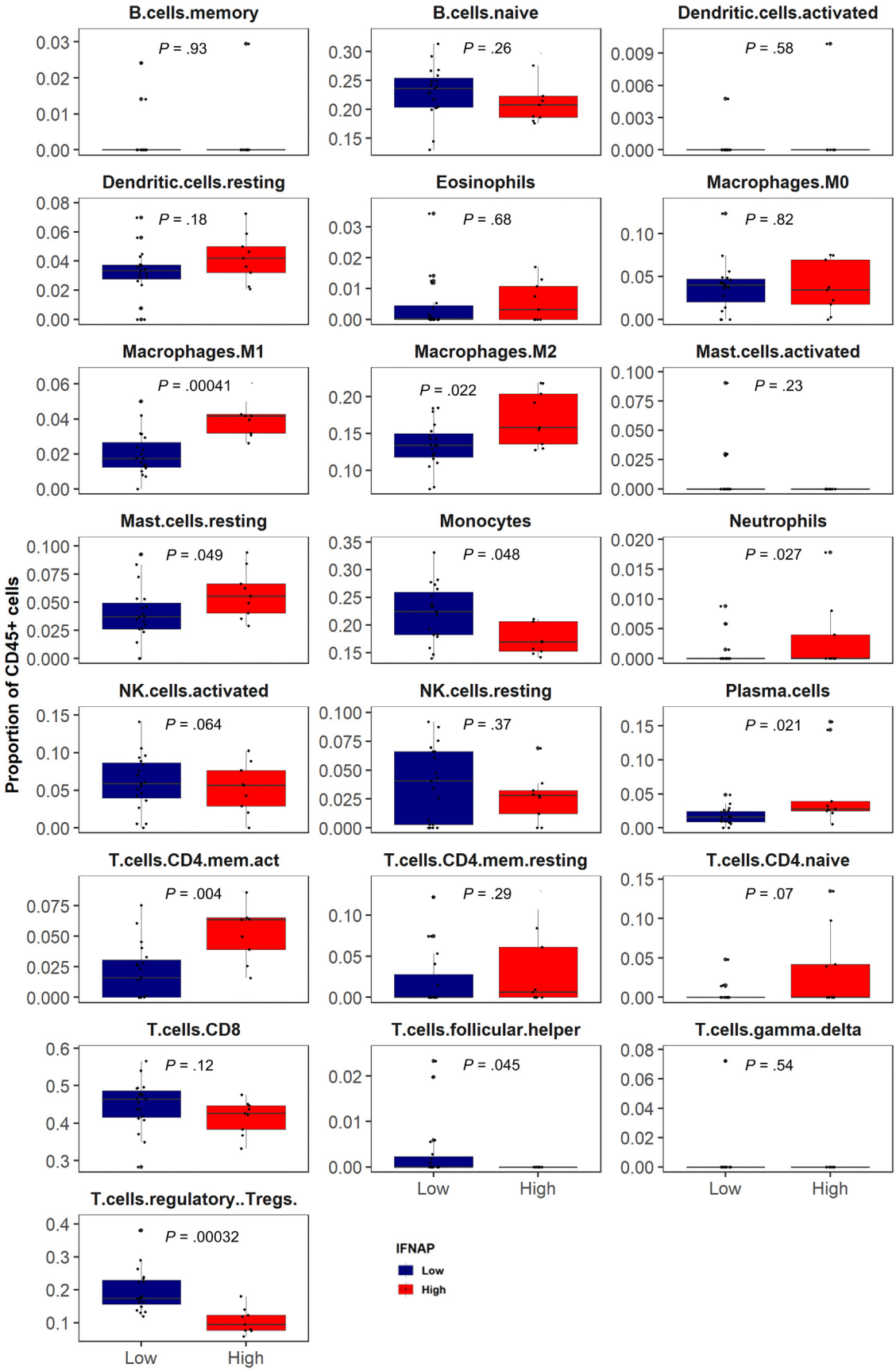

Supplementary Figure 9. Microenvironmental deconvolution with CIBERSORTx. Complete results of CIBERSORTx are shown based on expression of IFNAP. High expression was defined as the top tertile, whereas remaining patients were summarized as the Rest. Analysis was performed with 100 permutations in batch-correction mode. *P* values represent Wilcoxon rank-sum tests.

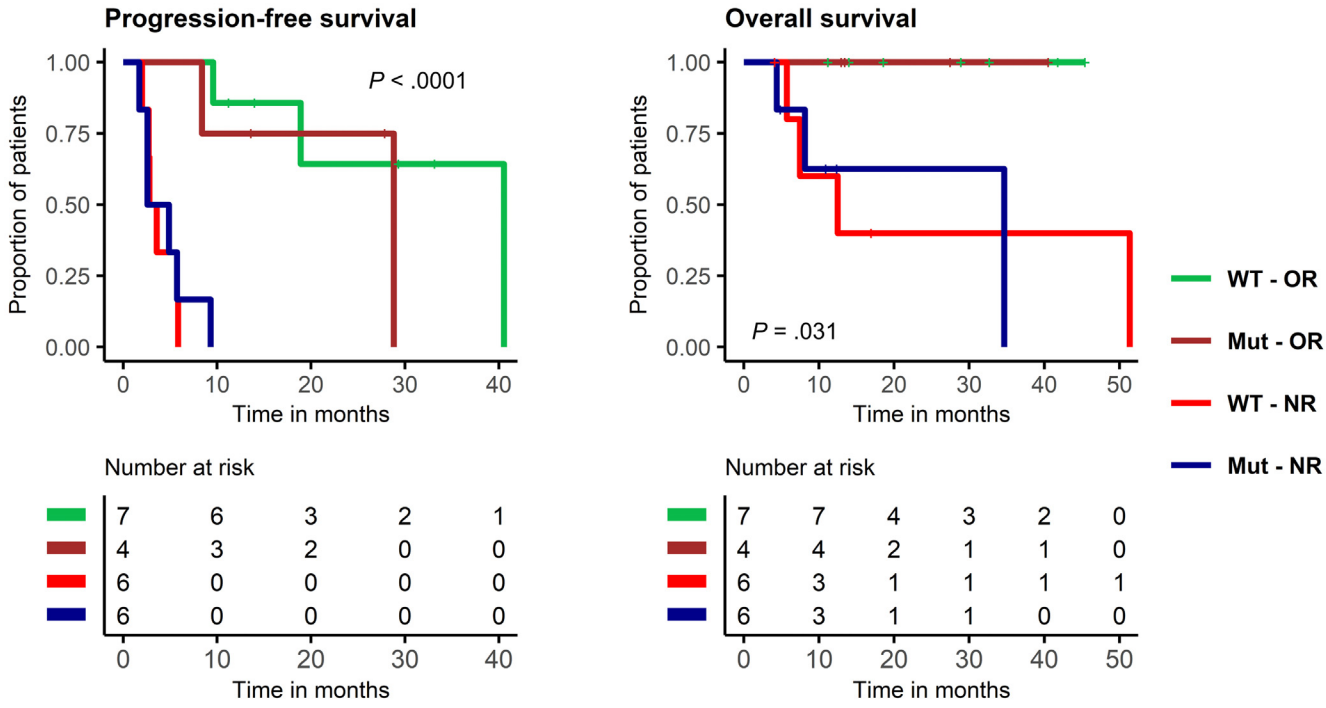

Supplementary Figure 10. Outcomes according to CTNNB1 mutational status. Kaplan-Meier estimates for PFS and OS are shown for patients treated with anti-PD1 in frontline. Although responders had markedly longer PFS and OS than non-responders, no differences were observed when comparing responders based on CTNNB1 mutational status. Likewise, outcomes of nonresponders were similar as well between CTNNB1-mutated cases and CTNNB1 wild-type (WT) patients. *P* values represent a log-rank test.

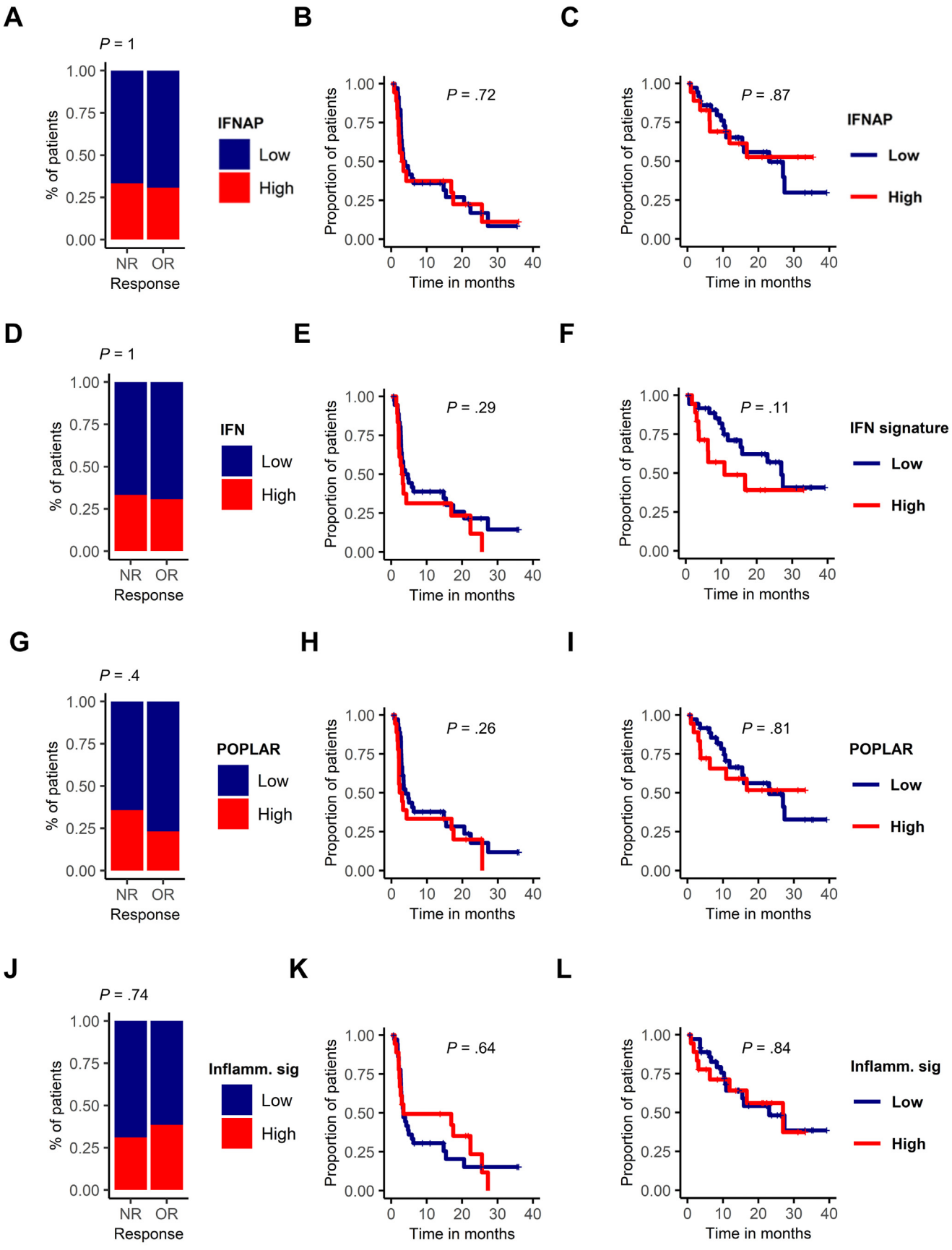
A
P = 1
% of patients
1.00
0.75
0.50
0.25
0.00
NR OR
Response
IFNAP
Low
High
B
P = .72
Proportion of patients
Time in months
C
P = .87
IFNAP
Low
High
D
P = 1
IFN
E
P = .29
F
P = .11
IFN signature
G
P = .4
POPLAR
H
P = .26
I
P = .81
J
P = .74
Inflamm. sig
K
P = .64
L
P = .84

Supplementary Figure 11. Performance of response signatures in patients treated with anti-PD1 after previous TKI therapy. Correlations between response signature expression, according to the top tertile vs remaining cases, and ORRs as well as Kaplan-Meier estimates for PFS and OS are shown for patients treated with anti-PD1 therapy in either second or third line in our dataset. Neither IFNAP nor previously reported signatures of response were able to predict any differences in ORR (*A*, *D*, *G*, *J*), PFS (*B*, *E*, *H*, *K*), and OS (*C*, *F*, *I*, *L*). The lack of discriminatory ability by these signatures suggests that previous TKI therapy can reshape the tumoral microenvironment to render initially inflamed tumors no longer amenable to anti-PD1 therapy. *P* values in χ^2 tests represent a 2-sided significance level.

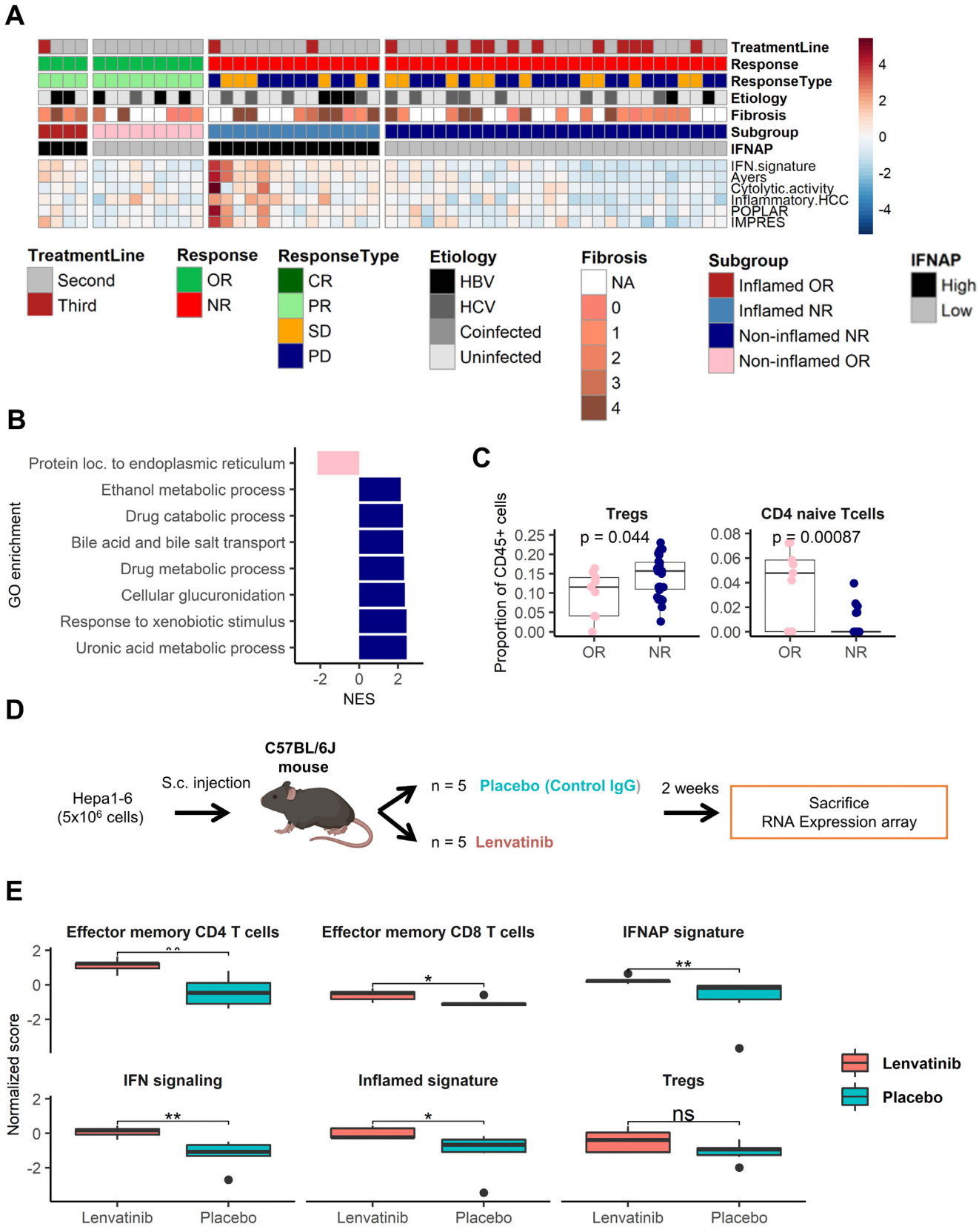
A
TreatmentLine
Response
ResponseType
Etiology
Fibrosis
Subgroup
IFNAP
IFN.signature
Ayers
Cytolytic.activity
Inflammatory.HCC
POPLAR
IMPRES
4
2
0
-2
-4
TreatmentLine
Second
Third
Response
OR
NR
ResponseType
CR
PR
SD
PD
Etiology
HBV
HCV
Coinfected
Uninfected
Fibrosis
NA
0
1
2
3
4
Subgroup
Inflamed OR
Inflamed NR
Non-inflamed NR
Non-inflamed OR
IFNAP
High
Low
B
Protein loc. to endoplasmic reticulum
Ethanol metabolic process
Drug catabolic process
Bile acid and bile salt transport
Drug metabolic process
Cellular glucuronidation
Response to xenobiotic stimulus
Uronic acid metabolic process
GO enrichment
-2
0
2
NES
C
Tregs
p = 0.044
CD4 naive Tcells
p = 0.00087
Proportion of CD45+ cells
0.25
0.20
0.15
0.10
0.05
0.00
0.08
0.06
0.04
0.02
0.00
OR
NR
OR
NR
D
C57BL/6J mouse
Hepa1-6 (5x10^6 cells)
S.c. injection
n = 5 Placebo (Control IgG)
n = 5 Lenvatinib
2 weeks
Sacrifice
RNA Expression array
E
Effector memory CD4 T cells
Effector memory CD8 T cells
IFNAP signature
IFN signaling
Inflamed signature
Tregs
**
*
**
**
*
ns
Normalized score
2
0
-2
Lenvatinib
Placebo
Lenvatinib
Placebo

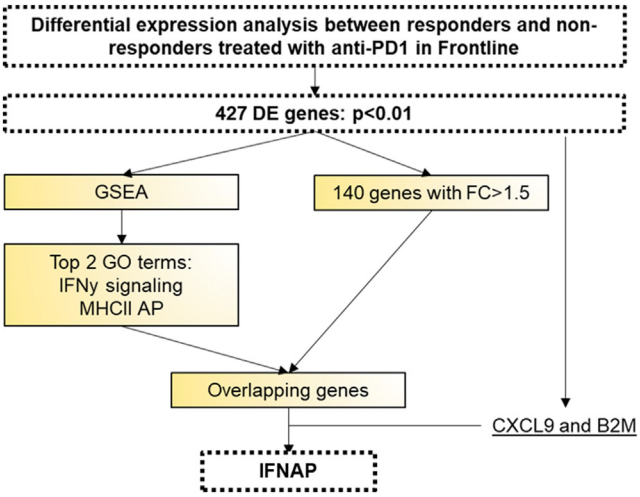

Supplementary Figure 13. Generation of IFNAP signature. IFNAP signature was created based on differential expression analysis using highly differentially expressed genes that overlapped with known Gene Ontology terms with the addition of CXCL9 and B2M.

Supplementary Figure 12. Prior TKI therapy interferes with the readout of inflammatory signatures as biomarkers of response. (*A*) Heatmap of patients treated with anti-PD1 in second and third line and previously characterized response signatures. (*B*) Depiction of normalized expression scores from Gene Ontology–based GSEA in patients with low IFNAP expression based on whether they responded (IFNAP low OR, pink) or not (IFNAP low NR, navy blue). (*C*) Boxplot representation of CIBERSORTx in patients with low IFNAP expression identifies severe Treg infiltration as an obstacle to achieve OR to anti-PD1 in patients treated in second and third line. (*D*) A previously reported murine model was re-analyzed to investigate the impact of TKI treatment via lenvatinib on the tumoral microenvironment. (*E*) In the murine model, lenvatinib elicited a shift in the cellular composition within the tumoral microenvironment and was able to augment inflammatory signaling. *P* values for Kaplan-Meier analysis derive from log-rank test, whereas those in the boxplot representation represent Wilcoxon rank-sum test.